Triarylisocyanurate-Based Fluorescent Two-Photon Absorbers

Yohan Gautier, Gilles Argouarch, Floriane Malvolti, Benjamin Blondeau, Nicolas Richy, Anissa Amar, Abdou Boucekkine, Krzysztof Nawara, Katarzyna Chlebowicz, Grażyna Orzanowska, et al.

Triarylisocyanurate-Based Fluorescent Two-Photon Absorbers

Yohan Gauthier,[a] Gilles Argouarch,[a] Floriane Malvolti,[a] Benjamin Blondeau,[a] Nicolas Richy,[a] Anissa Amar,[b] Abdou Boucekkine,[a] Krzysztof Nawara,[c] Katarzyna Chlebowicz,[c] Grażyna Orzanowska,[d] Marek Samoc,[e] Katarzyna Matczyszyn,[e] Marta Ziemianeck,[e] Mireille Blanchard-Desce,[f] Olivier Mongin,[a] Jacek Waluk,[c,d] and Frédéric Paul[a],*

Abstract: The synthesis and characterization of six triarylisocyanurates, featuring 2,7-fluorenyl or 9,10-anthracenyl groups incorporated in their peripheral arms are reported. Photophysical studies reveal that these new octupolar derivatives are more fluorescent ($\Phi_F \geq 0.60$ for all new compounds except **3**) and present a red-shifted first absorption and emission compared to their known phenyl analogues of comparable size. Depending on the nature of the terminal substituent, fast intramolecular energy transfer among the three arms or localization of the excitation on a single branch occurs after population of their first singlet excited state, the latter effect being only observed for strongly electron-releasing substituents in polar media. These new chromophores are also better two-photon absorbers than the 1,4-phenylene-based isocyanurates reported so far ($\sigma_2 \geq 500$ GM at 770 nm for **4-NPh$_2$**, **13** and **14**). All these spectroscopic features, analyzed with the help of quantum chemical calculations, are determining for stimulating the design of new biphotonic fluorescent dyes.

Introduction

Triaryl-1,3,5-triazinanes-2,4,6-triones (Isocyanurates) such as **1-X** are cyclotrimeric compounds known since the pioneering work of Hofmann in 1870.[1] Their production takes usually place by cyclotrimerization of the corresponding isocyanates and can be achieved using different catalysts.[2] Their most common industrial use is in the chemistry of polymers,[3] more particularly in the processes of synthesis of polyurethane foams. However, as we have previously shown, given their octupolar symmetry (Scheme 1), they are also potentially attractive for various applications based on their second- and third-order nonlinear properties,[4] which have hardly been investigated up to now.[5],[6] In this respect, because of the key role played by fluorescent substances with high two-photon absorption (2PA) cross-sections in bio-imaging,[7] we have decided to attempt developing isocyanurates possessing these two characteristics.

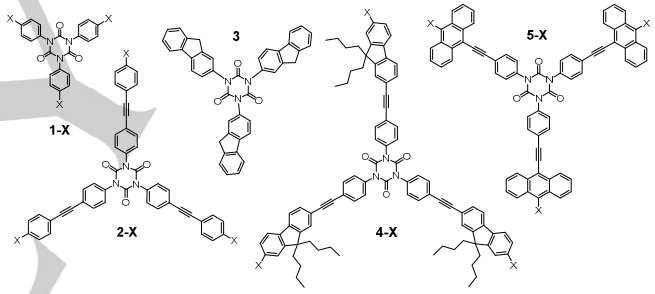

Scheme 1. Molecular structures of previously reported and currently targeted compounds.

We could previously show that isocyanurates with extended arms, such as **2-X** (Scheme 1) can be fluorescent and constitute fairly good two photons absorbers when functionalized by electron-releasing X substituents.[6a] In order to gain more insight into the structural modifications that can simultaneously favour fluorescence and 2PA, we have now synthesized and studied new derivatives presenting related structures. We thus explore herein the effect of replacing the peripheral phenyl rings by either 2-fluorenyl, 9,9-dibuyl-2-fluorenyl or functional 9,9-dibuyl-2,7-fluorenyl groups (**3** and **4-X;** ; X= H, NPh_2) or by functional 9,10-anthryl groups (**5-MEM**), as well as further extensions of the peripheral branches of these systems by 4-ethynyldiphenylaniline substituents, because 2-fluorenyl or 9,10-anthryl units are well known to favor 2PA and fluorescence.[8]

Results

Synthesis

[a] Y. Gauthier, Dr. G. Argouarch, Dr. F. Malvolti, N. Richy, Dr O. Mongin, Dr F. Paul, Prof. A. Boucekkine
Univ Rennes, CNRS, ISCR (Institut des Sciences Chimiques de Rennes), UMR 6226, 35000 Rennes (France)
Tel: (+33) 02-23-23-59-62
E-mail: frederic.paul@univ-rennes1.fr
[b] Dr. A. Amar,
Département de Chimie, Faculté des Sciences
Université Mouloud Mammeri
15000 Tizi-Ouzou (Algeria)
[c] Dr. K. Nawara, K. Chlebowicz; Prof. J. Waluk
Faculty of Mathematics and Science
Cardinal Stefan Wyszyński University
01-815 Warsaw (Poland)
E-mail: jwaluk@ichf.edu.pl
[d] G. Orzanowska, Prof. J. Waluk
Institute of Physical Chemistry
Polish Academy of Sciences
Warsaw (Poland)
[e] Dr. K. Matczyszyn, M. Ziemianek.
Advanced Materials Engineering and Modelling Group
Wroclaw University of Science and Technology
50-370 Wroclaw
[f] Dr. M. Blanchard-Desce
ISM, CNRS (UMR 5255)
Université Bordeaux
33400 Talence (France)

Supporting information for this article is given via a link at the end of the document.

The new cyclotrimer **3** was isolated in one step from commercial 2-fluorenyl isocyanate in good yields (53%) by catalytic cyclotrimerisation following a workup previously developed by some of us (Scheme 2).[6a]

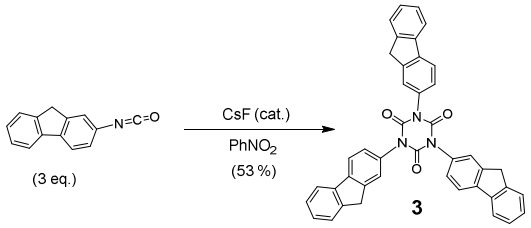

Scheme 2. Synthesis of **3**.

To access isocyanurates featuring an extended π-manifold, two alternative synthetic approaches had also been previously tested (Scheme 3). Sonogashira coupling reactions were used each time, starting either from the tri(4-bromophenyl)-isocyanurate precursor **1-Br** (route A) or from the triyne precursor **6** (route B).[9] When the corresponding arylalkyne is easily available, route A should be favored over route B, because the precursor **6** is obtained in two steps from the precursor **1-Br** in only 37% yield, whereas **1-Br** is conveniently obtained at the gram scale in one step (88% yield) from commercial 4-bromophenyl isocyanate *via* a catalytic cyclotrimerisation.[6a]

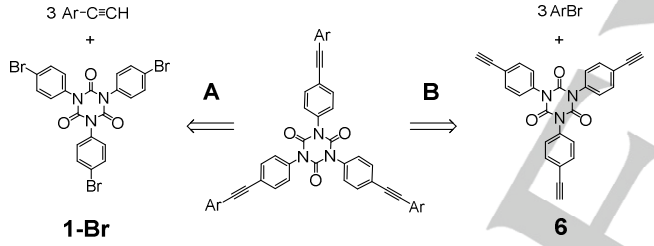

Scheme 3. Synthetic routes toward isocyanurates with extended π-manifolds.

Subsequently, the reaction between the **6** and the commercial 2-bromo-9,9-di-*n*-butyl-fluorene allowed straightforward isolation of the desired tris(2-fluorenyl)isocyanurate **4-H** (route B), while the diphenylamino analogue **4-NPh$_2$** was isolated following the alternative approach (route A) from **1-Br** and from excess of the alkyne **7** (Scheme 4). The synthesis of **7** was performed in two steps from known compound **8**[10] *via* **9** in *ca.* 60 % overall yield (Scheme 5). The IR and NMR signatures of the deprotected product **7** resemble those reported for its known diethyl analogue.[11]

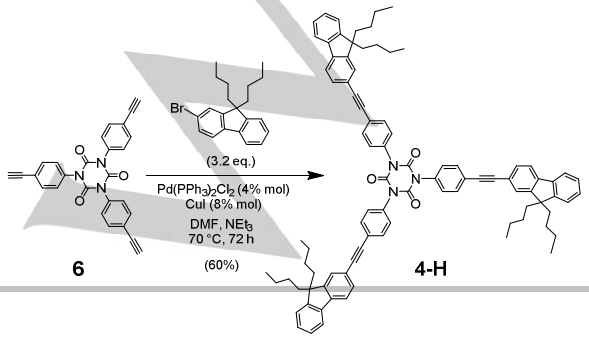

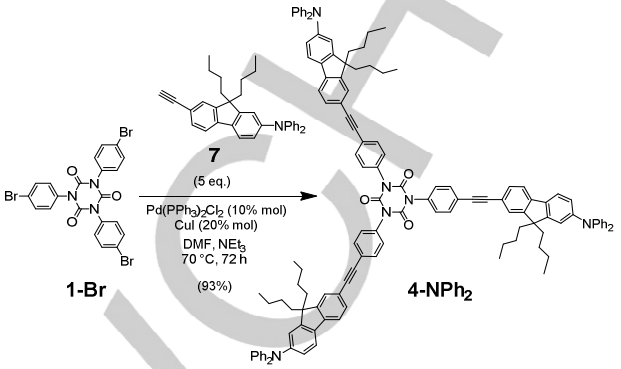

Scheme 4. Syntheses of the **4-X** derivatives (X = H, NPh$_2$).

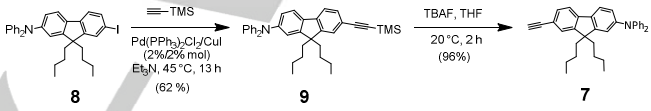

Scheme 5. Synthesis of **7**.

We next tried to isolate the corresponding 9,10-anthacenyl analogues **5-X**. After repeated failures to isolate any **5-H** from **1-Br** and 9-ethynylanthracene (route A), we attempted the alternative approach. However, reaction between **6** and 9-bromoanthracene (route B) proved not more rewarding. After each attempt, intractable and nearly insoluble crude solids (possibly mixtures) were obtained. Surmising that these issues resulted from solubility issues with the targeted **5-H** or one of its partially substituted analogues formed during the reaction "en route" toward **5-H**, we decided to use a more soluble anthracene reactant. Thus, the precursor **10** functionalized with a methoxy-ethoxymethyl substituent in position 9 was used. It was reacted with **1-Br**. The presence of the polyether tail on **10** and the use of DMF as co-solvent greatly helped performing the coupling reaction under homogeneous conditions, leading to the successful isolation of the desired cyclotrimer **5-MEM** in very good yields (90%). *via* route A (Scheme 6). Likewise to the previous reaction leading to **4-NPh$_2$**, rather high loadings of Pd(II) catalyst (10%) were required to speed up the coupling step. Comfortingly, **5-MEM** turned out to be soluble in most organic solvents.

The synthesis of the alkyne precursor **10** was performed in *ca.* 24 % yield from 9,10-dibromoanthracene *via* an original protocol in three steps based on a stepwise (one pot) electrophilic trapping reaction followed by a Corey-Fuchs reaction[12] (Scheme 7). During this reaction sequence, the structural changes between **11** and **10** were monitored by IR, which revealed the disappearance of the υ(C=O) vibrational mode around 1668 cm^{-1} for **11**, and the appearance of additional

υ(C≡C) and υ(≡C-H) stretching modes at 2055 and 3230 cm^{-1}, respectively, for **10**.

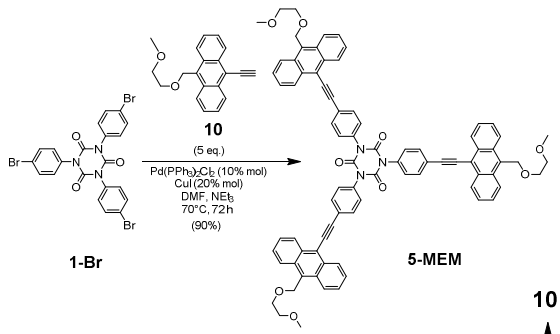

Scheme 6. Synthesis of **5-MEM**.

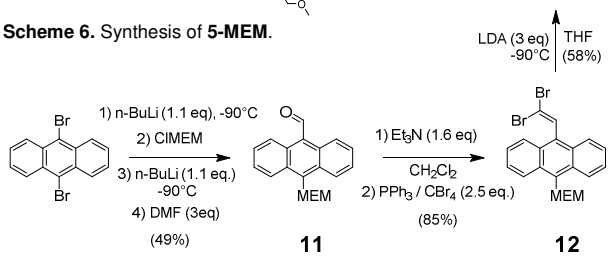

Scheme 7. Synthesis of **10**.

Finally, we also attempted isolating the extended versions of compounds **4-NPh₂** and **5-MEM** (*i.e.* **13** and **14**, respectively) by either coupling **6** with the iodofluorene derivative **15** (Scheme 8) or by reacting **1-Br** with the alkyne **16** (Scheme 9). The new halogenated precursor **15** was obtained from the diiodofluorenyl precursor in one step (Scheme 10), while the alkyne precursor **16**, needed for the second reaction, was obtained according to an experimental protocol analogous to that previously used to isolate **10** (Scheme 11).

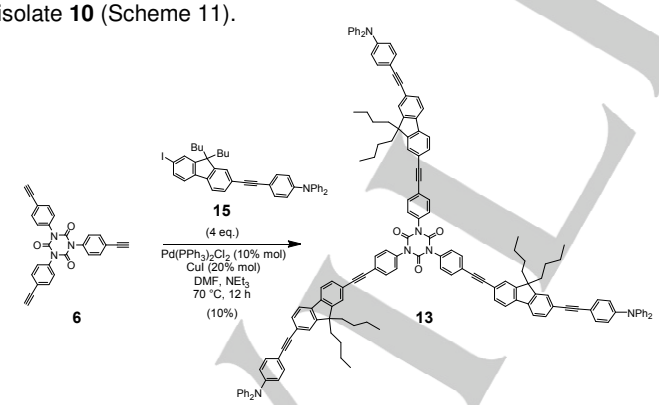

Scheme 8. Synthesis of **13** from **6** and **15**.

The former of these reactions led to isolation of the extended cyclotrimer **13** in a pure state, but in very low yields, after chromatographic separation. The second reaction leading to the extended cyclotrimer **14** was even more sluggish. It led to a mixture of products which proved difficult to purify. A fraction containing dominantly the desired compound (**14**) along with minor amounts of di- (**19**) and monocoupled product (**20**) was isolated by repeated chromatographic separations (MS evidence), from which minute amounts of **14** could be eventually isolated in the pure state (≤10%). The di- (**19**) and mono-coupled (**20**) compounds could not be separated from the mixture but were characterized by mass spectrometry. All other isocyanurates derivatives were fully characterized by IR and $^{1}H/^{13}C$ NMR spectroscopies, which allow observation of diagnostic signatures for these new compounds (Table 1).

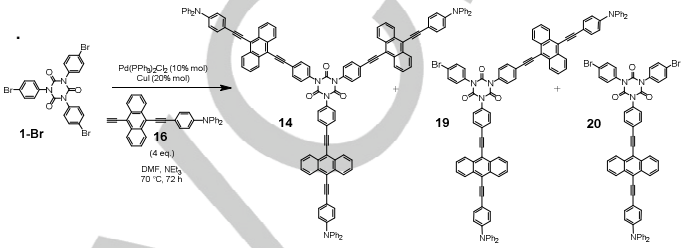

Scheme 9. Synthesis of **14** from **1-Br** and **16**.

Table 1. Characteristic spectral signatures of the new isocyanurates.

Cpnd	$\bar{\upsilon}_{(C\equiv C)}$ [a] [cm^{-1}]	$\bar{\upsilon}_{(C=O)}$ [a] [cm^{-1}]	$\delta_{(C\equiv C)}$ [b] [ppm]	$\delta_{(C=O)}$ [b] [ppm]
2-NPh₂ [c]	2209	1772,1718	91.7, 88.0	148.7
3	/	1771,1710	/	149.6
4-H	2203	1777, 1720	92.8, 88.9	148.4
4-NPh₂	2198	1778, 1720	93.0, 88.8	148.9
5-MEM	2192	1772, 1713	100.5, 88.4 [d]	148.7 [d]
13	2195	1778, 1717	92.4, 90.5, 89.8, 88.7 [d]	148.7 [d]
14	2183	1772,1720	103.4, 100.9, 88.3, 85.9	148.4

[a] FTIR in KBr pellet. [b] $^{13}C\{^{1}H\}$ NMR in $CDCl_3$ unless specified. [c] Data from ref. [6a]. [d] In CD_2Cl_2.

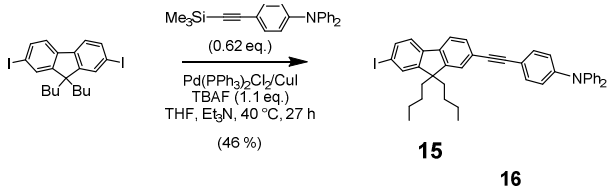

Scheme 10. Synthesis of **15**.

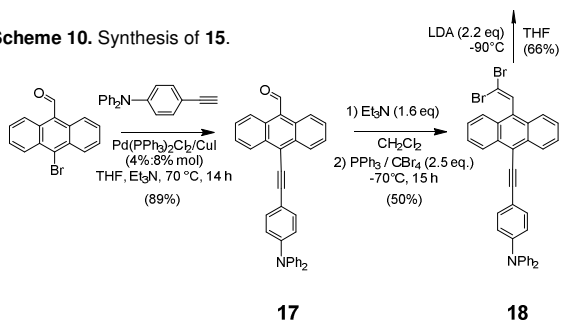

Scheme 11. Synthesis of **16**.

Table 2. Photophysical data for the new isocyanurates *vs.* those for known isocyanurates.

Cpnd	λ^{max}_{abs2} [nm]	ε_{max2} [10^3.cm^{-1}.M^{-1}]	λ^{max}_{abs1} [nm]	ε_{max1} [10^3.cm^{-1}.M^{-1}]	λ^{max}_{em} [nm]	Φ_F[a]	Stokes shift [b] [cm^{-1}]	DFT [c] λ^{max} [nm] [*f*]	Ref.
1-H	/	/	256	0.9	283	0.005	2747	202 [0.12] 202 [0.12]	This work and [6a]
2-H	<240	-	304	90.5	312	0.037	843	272 [1.81] 272 [1.81]	This work and [13]
2-NPh$_2$	294	56	364	99.0	437	0.73	4589	404[1.95] [d] 404[1.95] [d]	[6a , 14]
3	270	73	302, 318 (sh)	38.3	305	0.25	35	269 [1.15] 269 [1.15]	This work
4-H	<240	-	344	101.0	355	0.60	900	345 [2.83] 345 [2.81]	This work
4-NPh$_2$	308	85	383	129.0	463	0.78	4511	404 [2.30] 404 [2.35]	This work
5-MEM	306	57	431	69.0	437	0.72	318	449 [1.00] 449 [1.02]	This work
13	316	99	376	186.0	469	0.62	5274	433 [3.28] 433 [3.52]	This work
14	277	124	486	86.0	589	0.80	3683	561 [2.37] 561 [2.36]	This work

All wavelengths are given ± 2 nm and all absorption coefficients ± 1000 M^{-1}.cm^{-1}. [a] Fluorescence quantum yield (±10%) in CH_2Cl_2 when excited at λ_{abs} (Standard : quinine bisulfate in H_2SO_4 0.5 M). [b] Stokes shift = ($1/\lambda_{abs}$ - $1/\lambda_{em}$). [c] Calculated at the MPW1PW91/6-31G* level on computationally-simpler model complexes (see below) in CH_2Cl_2 (*f* = oscillator strength). [d] 340 [2.50] and 340 [2.50] when calculated at the CAM-B3LYP/6-31G* level in CH_2Cl_2.[14]

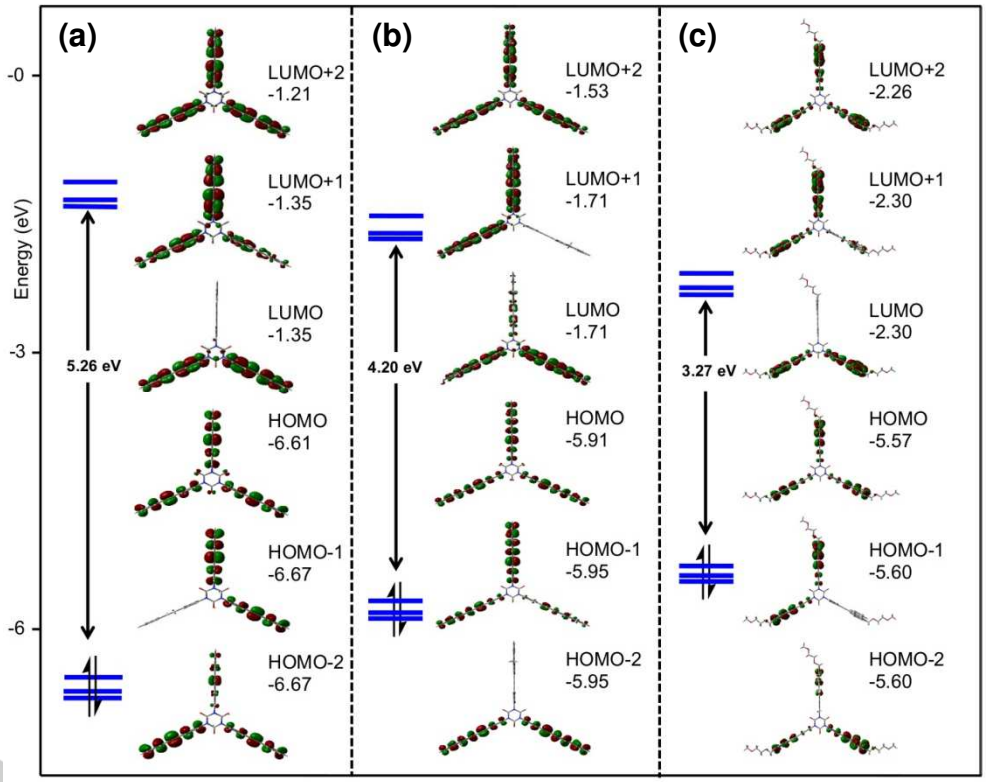

Figure 1. Frontier molecular orbitals involved in the lowest-energy (intense) allowed transition for **2-H** (a), **4-H'** (b) and **5-MEM** (c) (isocontour 0.03 [e/bohr^3]$^{1/2}$).

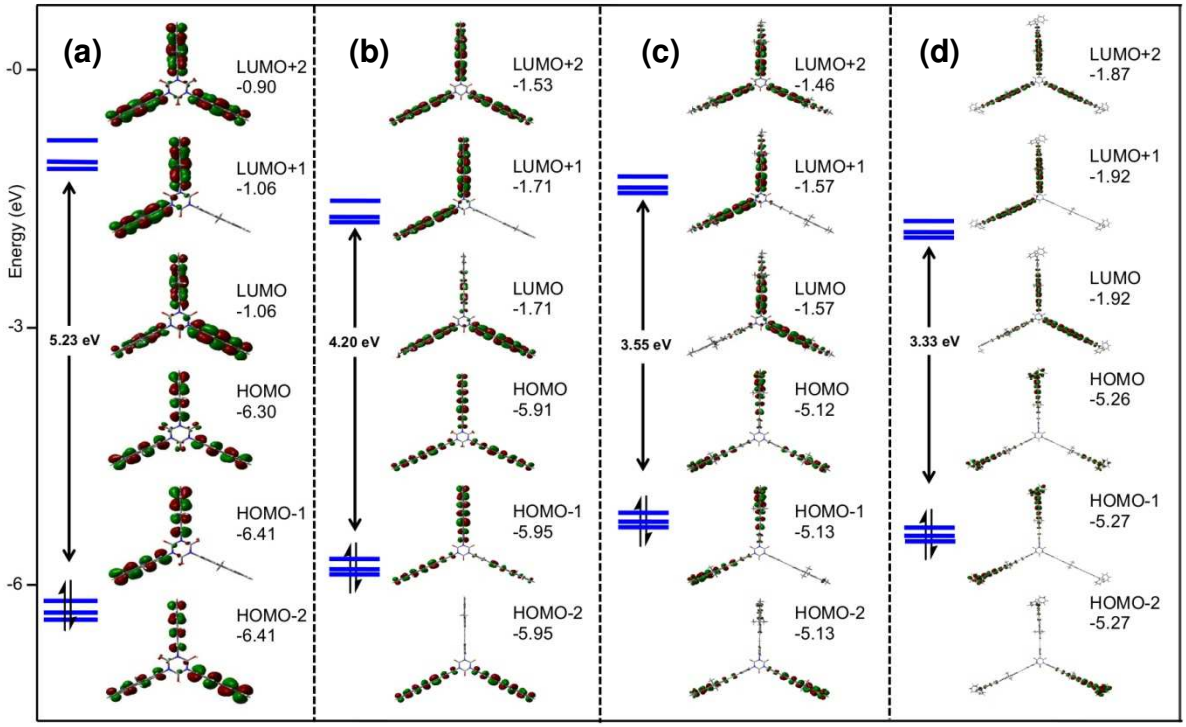

Figure 2. Frontier molecular orbitals involved in the lowest-energy (intense) allowed transition for **3** (a), **4-H'** (b), **4-NMe$_2$"** (c) and **13"** (d) (isocontour 0.03 [e/bohr^3]$^{1/2}$).

Electronic Absorption and Emission

The linear photophysical properties of the new isocyanurates were next determined by measuring their electronic absorption and emission spectra (Table 2).

Regarding the fluorene-containing derivatives **3**, **4-H**, **4-NPh$_2$** and **13**, these measurements reveal similar trends between these molecules to those previously established between **1-X** and **2-X** relatives.[6a] Thus, extension of the π-manifold on the three peripheral branches red-shifts the first absorption band. For instance, the compound **3**, when compared to its phenyl analogue **1-H**, exhibits bathochromic a shift of *ca.* 7615 cm^{-1} for this band. Similar to what had been observed for **1-H**, the first absorption at *ca.* 318 nm appears as a very weak shoulder overlapping a stronger (and structured) band at higher energy. The latter located near 292-302 nm resembles a fluorene-based $\pi^*\leftarrow\pi$ band. Finally, a third unstructured and more intense band at 270 nm dominates the absorption pattern below 250 nm. This band looks like the typical $\pi^*\leftarrow\pi$ band traditionally observed for such cyclotrimers.[6a] Upon progressing to **4-H**, a further shift of the former absorption to low energy takes place, giving rise to an intense and structured band which possibly hides the weaker transitions previously observed as a shoulders for **3**.

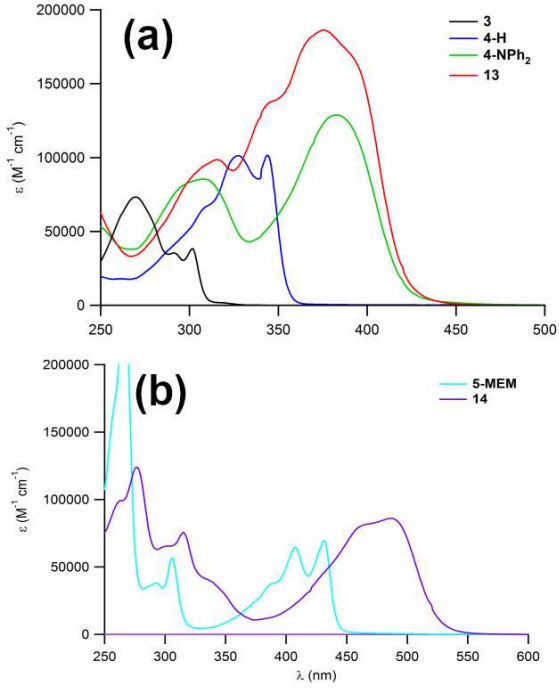

Figure 1. UV-vis spectra for (a) **3**, **4-X** (X = H, NPh$_2$) and **13** or (b) **5-MEM** and **14** in CH_2Cl_2 (20 °C).

As stated for **2-X** derivatives,[6a] replacing the 4-proton in **4-H** by an electron-releasing substituent also produces a red shift of the first absorption band. The substituent-induced shift of the first absorption is less pronounced in **4-X** derivatives than in **2-X** derivatives. It remains slightly larger than that observed between **4-NPh$_2$** and **13**, which is associated with the extension of the π-manifold on the peripheral arms. A second absorption, at lower energy, is also present at 308 nm for **4-NPh$_2$** (Figure 1). Progressing to the largest compound of this series (**13**) also results in an increase of the absorption coefficient of these bands, still in line with the extension of the π-manifold. Notably, the second absorption of **13**, while being more intense than that in **4-NPh$_2$**, is also red-shifted. Similar trends are observed for the 1,9-antharcenyl derivatives **5-MEM** and **14** (Figure 1b), but the effects are overall less pronounced than for the fluorenyl derivatives (Figure 1a).

In line with our initial goals, all these new compounds are luminescent, with quantum yields sufficiently high for imaging purposes ($\Phi_F \geq 0.15$). Likewise to the improvement in fluorescence quantum yield previously stated when proceeding from **1-H** (0.005) to **2-H** (0.037) and to **2-NPh$_2$** (0.73), a related increase (Table 2) takes place when progressing from **3** (0.19) to **4-H** (0.60) to **4-NPh$_2$** (0.78). However, moving to the largest compound of this series (**13**) does not result in a further increase of the fluorescence quantum yield (0.62). Also, compared to the emission of **4-H**, those of **4-NPh$_2$** and **13** have lost their fine structure (see ESI, Figure S17). For all these compounds, the red shift of the emission band mirrors that of their first absorption band.

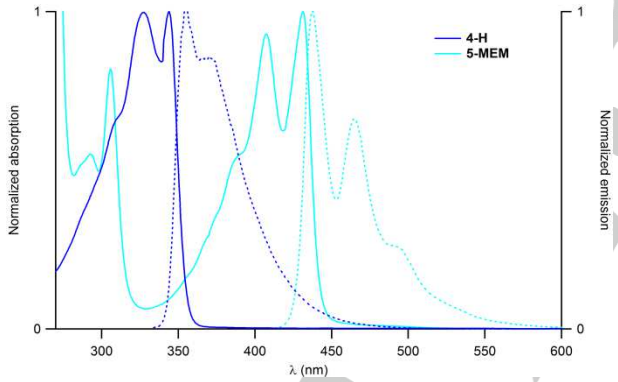

Figure 2. Normalised absorption and emission UV-vis spectra **4-H** and **5-MEM** in CH_2Cl_2 (20 °C).

Then, regarding **5-MEM** and **14** (Figure 1b), both compounds also appear to be strongly luminescent (Table 2). Compared to **4-H**, the lowest transition of **5-MEM** is red shifted by more than 88 nm, both in absorption (*ca.* 5870 cm^{-1}) and emission (*ca.* 5290 cm^{-1}). **5-MEM** is also much more fluorescent than **4-H** and **2-H** (Φ_F = 0.72 *vs.* 0.60 and 0.037, respectively), exhibiting structured emission bands with a vibronic progression of *ca.* 1380 cm^{-1}, which possibly corresponds to an δ_{CH2} mode.[15] This emission takes place at the same wavelength than that of **2-NPh$_2$** and presents a similar fluorescence quantum yield. Its expanded parent (**14**) presents a further red-shift of its emission (*ca.* 5900 cm^{-1}) and an improved emission quantum yield (Φ_F = 0.80) compared to **5-MEM** (Φ_F = 0.72).

Finally, from the data gathered from the various mixtures of **14**, **19** and **20** that were isolated, it appears that the bis- and mono-substituted derivatives **19** and **20** have their first absorption and emission bands at very similar energies than those of their octupolar parent **14**, an observation confirmed by DFT calculations (see below).

Solvatochromism and Polarized Fluorescence

To understand better the origin of the fluorescence observed for these compounds, we have undertaken solvatochromism and polarized fluorescence studies on **2-NPh$_2$**, **4-H**, **4-NPh$_2$** and **5-MEM** (Table 3).

Table 3. Solvent-dependent spectral and photophysical parameters of **2-NPh$_2$**, **4-H**, **4-NPh$_2$** and **5-MEM** at 25 °C.

Solvent	λ^{max}_{abs} [a] [nm]	ε_{max} [b] [M^{-1}.cm^{-1}]	λ^{max}_{em} [c] [nm]	Φ_F [d]	τ [e] [ns]
2-NPh$_2$					
n-Hexane	359	72000	382	0.38	2.60 [f]
CH_2Cl_2	364	99000	437	0.76	/
MeOH	358	120000	443	0.50	1.95
CH_3CN	357	101000	457	0.65	2.90
1-BuOH	359	92000	422	/	/
1,4-Dioxane	358	124000	409	/	/
4-H					
n-Hexane	342	126000	346	0.88	1.10
CH_2Cl_2	344	102000	355	0.72	/
MeOH	341	142000	348	0.68	0.90
CH_3CN	341	126000	351	0.81	0.75
MTHF	342	/	352	/	/
PrOH	342	/	352	/	/
4-NPh$_2$					
n-Hexane	376	134000	401	0.63	1.10
CH_2Cl_2	383	129000	463	0.83	/
MeOH	376	/	466	0.71	1.90
CH_3CN	378	124000	488	1.00	2.30
1-BuOH	379	136000	445	/	/
1,4-Dioxane	376	115000	423	/	/
5-MEM					
Toluene	432	52000	438	0,73	1.10
n-Hexane		/	423	/	/
CH_2Cl_2	431	69000	435	0.76	/
MeOH	427	/	432	0,51	3.50
CH_3CN	428	64000	433	0,68	3.30

All wavelengths are given ± 2 nm and all absorption coefficients ± 1000 M^{-1}.cm^{-1}. [a] Maximum of the first absorption band. [b] Absorption coefficient of the first absorption band. [c] Fluorescence maximum. [d] Fluorescence quantum yield (±10%). Note that these values are slightly different (within experimental uncertainty) than those given in Table 2, which were derived under different conditions. [e] Fluorescence decay time. [f] Biexponential decay: the shorter decay (0.8 ns) is most likely due to an aggregate.

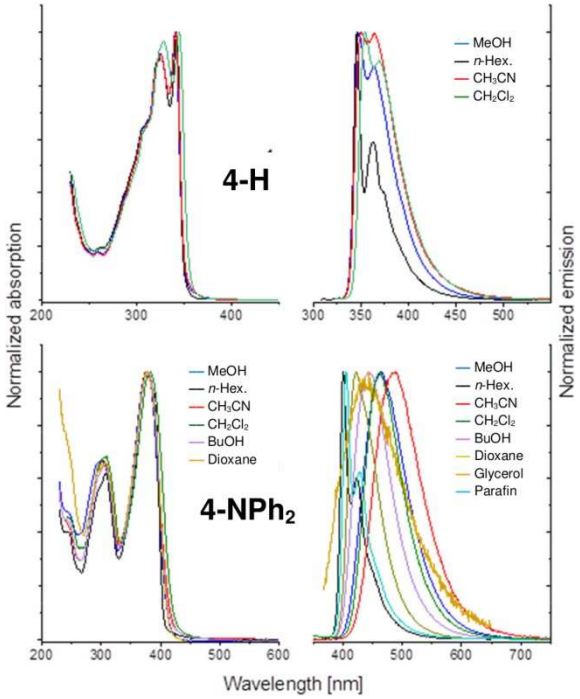

Figure 3. Absorption (left) and fluorescence (right) spectra of **4-H** (top) and **4-NPh$_2$** (bottom) in different solvents at 293 K (20 °C).

From our studies (Table 3), it appears that the first allowed absorption of these derivatives is weakly, if at all, affected by solvent polarity. In line with DFT computations (see later), this confirms the lack of dipole moment in the ground state (GS). Indeed, their threefold symmetry implies either a zero dipole moment, or a dipole aligned along the C_3 symmetry axis. An in-plane dipole moment is possible only for the less symmetrical conformations or for unsymmetrical derivatives such as **19** (see later). In contrast to absorption studies, different fluorescence patterns are observed for different molecules. In **4-H** and **5-MEM**, the emission remains practically the same in nonpolar and polar environments, whereas this is not the case for **4-NPh$_2$**. Likewise to what was already observed previously for **2-NR$_2$** derivatives (R = NH$_2$, NMe$_2$, NPh$_2$),[6a] large solvatochromic shifts are found in the more polar solvents: the emission maximum moving to lower energy upon increasing the polarity of the surrounding medium. This indicates a dipole moment larger in the excited state than in the GS, and thus, deviation from a threefold symmetry in S_1 (we exclude a special, improbable case of a significant dipole moment increase along C_3). An instructive comparison is presented by the behavior of **4-H** and **4-NPh$_2$** (Figure 3). Solvatochromic shifts are barely observed in the former, but become quite pronounced when the fluorene moiety is substituted with an electron-donating diphenylamino substituent. On the other hand, no solvatochromic effects are observed for **5-MEM**, a molecule functionalized with a poorly electron-releasing substituent on its peripheral anthracene rings (Figure 4). Such substituent-dependent solvatochromic behavior is usually characteristic of localization of the excitation in one arm of these octupolar derivatives.[16]

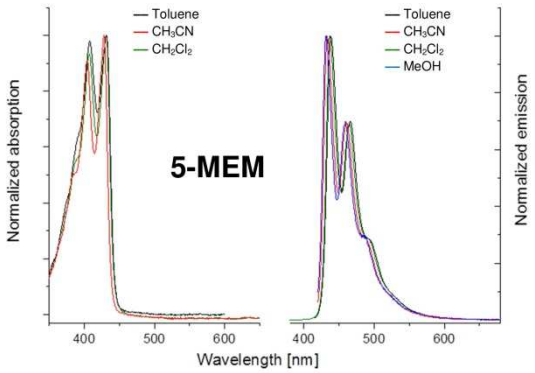

Figure 4. Absorption (left) and fluorescence (right) spectra of **5-MEM** in different solvents at 293 K (20 °C).

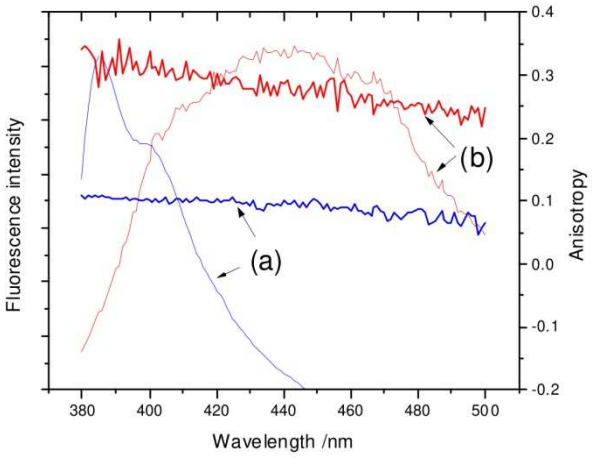

Figure 5. Fluorescence anisotropy of **4-NPh$_2$** measured at 273 K in (a) liquid paraffin and (b) glycerol.

In order to address this issue, we have measured the fluorescence anisotropy in both polar and nonpolar environments (Figure 5).[17] Viscous solvents, glycerol and paraffin have been used for this purpose, in order to prevent depolarization by rotational relaxation. Large size of the molecules combined with a short S_1 lifetime significantly reduces this effect. The observed anisotropy values (Figures 5) are very different for polar and nonpolar solvents. In the former set, values close to 0.4 are observed, characteristic for parallel orientation of transition moments responsible for absorption and emission. On the contrary, the anisotropy values in paraffin are only slightly lower than 0.1, which is the value expected when any transition moment direction in a molecular plane is possible. These results not only confirm the conclusion about the localization of excitation in polar environments: they also demonstrate that, for the same molecule in a nonpolar environment, the excitation "hops" between the three moieties during the lifetime of the excited S_1 state. Indeed, the latter phenomenon results in an efficient loss of the polarization of the

incoming light during emission. In contrast, instant solvation of the excited sate in a polar solvent, concomitantly to localization of the excited state in one arm, ensures a better preservation of the polarization of the incoming light. Naturally, this is easier to achieve when large dipole moments are induced in the excited state. Accordingly with our findings, this explains why the polarization of the emitted light (i.e. requiring localization of excitation) is highest for the compounds bearing the most electron-releasing substituents such as diphenylamino groups in polar solvents. In **4-H** and **5-MEM** which do not exhibit solvatochromism, low anisotropy values (≈ 0.1) are observed in both polar and nonpolar solvents, indicating fast transfer of excitation between the three branches in their first singlet excited state.

The Lippert-Mataga[18] plots obtained from these measurements for **4-NPh$_2$** and **2-NPh$_2$** in solvents of varying polarity do not exhibit a perfect linearity (ESI, Figure S18). Such a deviation from linearity is often observed when specific H-bonding interactions take place between the alcohols and carbonyl oxygen atoms.[19] In accordance with such a possibility, the shifts between absorption and emission observed for alcohols seem to be lower than those observed for other solvents. These shifts further suggest a weakening of the H-bond upon excitation.

Biphotonic Absorption

Two-photon absorption (2PA) properties of most of these cyclotrimers were then determined by two-photon excited fluorescence (2PEF). For all these compounds, as revealed by overlaying the one-photon absorption spectrum plotted at twice their wavelength with the corresponding two-photon absorption spectrum, two-photon absorption appears to take place in the first absorption band (ESI, Figure S23). Albeit sufficiently fluorescent, several of them (**3**, **4-H**) could however not be measured on our setup due to the limited wavelength range of the exciting laser beam ($\lambda_{abs} \geq 480$ nm) and detector (700-1000 nm; $\lambda_{em} \geq 350$ nm). For these compounds and some of the others, open-aperture Z-scan measurements have been undertaken in order to determine their effective 2PA cross-sections. All the results are given in Table 4.

Among the compounds which were subjected to both techniques, except for the compound **5-MEM**, the match between the 2PA cross-sections derived by Z-scan and those derived by 2PEF can be considered as fair, given the large experimental uncertainty of the Z-scan measurements. In all cases, the effective cross-sections derived by Z-scan are larger than those found by 2PEF, as often observed in the literature.[20] In the specific case of compound **5-MEM** the effective cross-section is *ca.* one order of magnitude larger. This is unexpected and indicates that other phenomena than just 2PA come in play during the measurement. A common explanation is that excited state absorption (ESA) takes place from the 2-PA state under the Z-scan conditions.[20] Another possibility would be the occurrence of reverse saturable absorption (RSA) in addition to 2PA. This second possibility would be in line with the existence of a low-lying (dark) triplet state computed at 876 nm for this molecule (see ESI, Table S2). Among the molecules that were only subjected to Z-scan analysis (**3** and **4-H**), the effective 2PA cross-section derived for **4-H** can be considered as pure 2PA. It is indeed lower than that found for its more polarized analogue **4-NPh$_2$** and fairly well spectrally localized at a wavelength slightly below twice the wavelength of the maximum of the first absorption peak of **4-H** (620 nm), as was observed for the other compounds in this series. By comparison, the cross-section determined for **3** at 300 nm (which does not correspond to a real maximum) should be taken with much more caution, because 2PA takes place very near to the solvent cut-off. Actually, to dissolve this poorly soluble compound we had to use chlorobenzene as a solvent for Z-scan and this solvent starts absorbing around 290 nm.

Table 4. 2PA properties of selected derivatives by 2PEF or Z-scan in solution at 25 °C.

Cmpd	λ_{2PA} [a] [nm]	σ_2 [b] [GM]	$\sigma_{2\ eff}$ [c] [GM]	$\Phi_F.\sigma_2$ [d],[e] [GM]	$\Phi_F.\sigma_2/MW$ [e] [GM.g^{-1}]
2-NMe$_2$	720	360[6a]	/	72	0.091
2-NPh$_2$	740/710	410[6a]	410±30[21]	300	0.259
3	≤600	/	/[g]	/	/
4-H	640	/	200±20	120	0.095
4-NPh$_2$	770/720	500	850±150	390	0.222
5-MEM	700[h]/650	40[h]	750±50	29	0.023
	820/775	8	500±150	6	0.005
	850/850	5	25±50	4	0.003
13	770/725	540	1000±200	340	0.165
14	770	820	/	656	0.374
	940	280	/	224	0.126

[a] Wavelengths of the nonlinear absorption maxima determined in CH_2Cl_2 by 2PEF or in THF (unless specified) by Z-scan. [b] 2PA cross-sections (± 10%) at λ_{2PA}. [c] Effective 2PA cross-sections derived from Z-scan measurements in THF. [d] Two-photon brightness figure-of-merit for imaging applications.[8e] [e] Derived using σ_{2eff} only when σ_2 (2PEF) was not available. [f] Same as [d] corrected for the molecular mass (*MW*). [g] Effective 2PA cross-section were measured in 1,2-dichlorobenzene but no reliable cross-section could be found. [h] Maximum not detected.

The largest 2PA cross-sections is found for the extended derivative **14** (820 GM), but in this case this 2PA transition does not take place into the first excited state. Likewise to the second 2PA band of **5-MEM** (near 700 nm), the dependence of this 2PA band on the fluence of the incoming laser beam is quadratic (ESI; Figures S25b and S27b). This indicates the occurrence of a single biphotonic process, in line with pure two-photon absorption. Now, when only the first 2PA bands are considered (*i.e.* the most red-shifted ones), the 2PA cross-section record is held by the extended compound **13**. Again a quadratic dependency of the two-photon brillancy on the intensity of the laser beam can be established evidencing a pure 2PA phenomenon.

The two-photon brilliancies ($\Phi_F.\sigma_2$) indicate that **4-NPh$_2$** is the most fluorescent compound when excited by two-photons in its first excited state (around 770 nm) and that **14** will be the most fluorescent one of these series when two-photon excitation is

performed at wavelengths above 700 nm. Finally, when these two-photons brillancies are corrected for the increase in size of the underlying chromophore *via* their molecular mass, a practice often observed for deriving related figures of merit,[8e] it is still **4-NPh$_2$** and **14** that hold the record, meaning that these molecules present the best imaging potential among the new derivatives presently synthesized.[7]

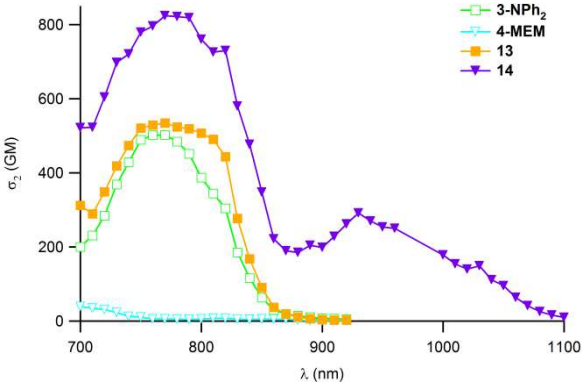

Figure 6. Two-photon absorption spectra for **3-NPh$_2$, 4-MEM, 13** and **14** in CH_2Cl_2 in dichloromethane (20 °C).

DFT Calculations

Density functional theory (DFT) calculations were performed on some of these derivatives (**3**, **4-H**, **4-NPh$_2$**, **5-MEM**, **13** and **14**). In compounds **4-X** and **13**, the *n*-butyl chains have been replaced by hydrogen atoms (**4-X'**) of by methyl groups (**4-X"** or **13"**) to speed up the calculations. In these compounds, as previously found for the **2-X** derivatives,[6a] the three peripheral arms adopt a slightly tilted conformation relative to the central phenyl plane after geometry optimization in CH_2Cl_2. In this respect, the sizable dipole moments computed for **3**, **4-H'**, **4-NMe$_2$"** and **13"** are almost perpendicular to the isocyanurate plane and result from this particular orientation of the fluorenyl-containing arms in these molecules (ESI; Figure S19).[22] For most compounds, given the low activation barriers around the single bonds on each side of the alkyne spacers,[23] these dipole moments will nearly vanish in solution at 25 °C, when free rotation of the arm is possible. Thus, in line with our measurements of solvatochromism, DFT calculations confirm that the dipole moment of these molecules is close to zero in the GS and will have an essentially null component in the molecular plane whenever sizeable (Table 5). In contrast an in-plane dipole moment of *ca.* 5.6 D is found for the non-symmetric isocyanurate derivative **19** in the GS.

The HOMO-LUMO gap in these three derivatives becomes smaller in the order **3** > **4-H'** > **4-NMe$_2$"** > **13"** > **5-MEM** > **14**, mirroring the trend in energies experimentally observed for the lowest-lying intense absorptions of these compounds (Table 5). Except for **3**, TD-DFT calculations reproduce fairly well the most intense transitions observed at lowest energy and confirm the observed increase in oscillator strength between these derivatives (Table 1). As previously observed for **1-X** and **2-X** derivatives, the lowest-energy transition calculated always corresponds to a symmetrical charge transfer between the periphery and the center, with a dominant $\pi^* \leftarrow \pi$ character ($E \leftarrow A$ under strict C_{3v} symmetry). Although the optimized GS structures do not belong to the C_{3v} symmetry group, the energetic degeneracy of the two first transitions and their spatial distribution recall those expected for an $E \leftarrow A$ transition under strict C_{3v} symmetry. The charge transfer occurs from the periphery towards the center, a trend which becomes more pronounced when X becomes more electron-releasing. The intense absorption at higher energy, observed near 300 nm with **4-NPh$_2$**, and **5-MEM**, also corresponds to an allowed $\pi^* \leftarrow \pi$ transition, but involves deeper lying occupied MOs (HOMO-3; see ESI). As a result, this transition is more arm-centered than the first one.

Table 5. Calculated dipole moments and HOMO-LUMO gaps in CH_2Cl_2 for selected derivatives (C_1 symmetry).

Cpnds	μ [D]	HOMO-LUMO gap [eV]	Refs
2-H	0.001	5.26	This work
2-NMe$_2$	0.63	3.61	[6a]
2-NPh$_2$	0.08	3.46	[6a]
3	2.40	5.23	This work
4-H'	0.80	4.20	This work
4-NMe$_2$"	2.10	3.55	This work
5-MEM	0.6	3.27	This work
13"	4.15	3.33	This work
14	0.04	2.66	This work
19	5.58	2.66	This work

For **3**, the two less intense transitions experimentally evidenced at lowest energy were not predicted by DFT and only the largest one at 256 nm, corresponding to the transition discussed above, was properly modelled. Most likely, the oscillator strength of these transitions was underestimated while their energy was overestimated by calculations, so that they remain "hidden" among the weaker excitations computed at higher energy for **3**. Finally, calculations for the non-symmetric derivative **19** reveal a very similar HOMO-LUMO gap than for its fully symmetric octupolar parent **14** and confirm that the first $\pi^* \leftarrow \pi$ absorption of both compounds should not be distinct on their UV-vis spectra.

Discussion

In this work, we show that fluorescent aromatic units, such as 2-fluorenyl or 1-anthracenyl, when incorporated at the periphery of the conjugated peripheral bridges allow imparting a significant fluorescence to the resulting isocyanates.

In spite of the increased length of the 2,7-fluorenyl linker compared to a 1,4-phenylene group, the electronic influence of the terminal substituent can still be felt by the isocyanurate central core, as exemplified by the bathochromic shift of the first absorption of **4-NPh$_2$** relative to **4-H**. Thus, a comparable 39 nm (2960 cm^{-1}) shift takes place upon progressing from **4-H** to **4-NPh$_2$** (to be compared with the 40 nm (5422 cm^{-1}) shift observed between **2-H** and **2-NPh$_2$**), revealing the existence of an actual electronic interaction between the diphenylamino group and the isocyanurate core through the π-manifold of the entire branch in **4-NPh$_2$**. Comparison with the corresponding **2-X** analogues reveals that part of the bathochromic shift stated for **4-X** derivatives is also attributable to the increased length of the π-manifold on each branch, not only to the substituent effect. Along the same lines, comparison between **5-MEM** and **4-H** reveals that replacement of the 2,5-fluorenyl linker by a 9,10-anthryl linker allows for a further red-shift of the first absorption and emission bands, accompanied by an improvement of the fluorescence quantum yield, and this in spite of the concomitant decrease in intensity of their first absorption band. When the data gathered for **13** and **14** are also considered, this trend appears to be quite general.

As previously established for the **2-X** derivatives,[6a] the first (allowed) excited state of triarylisocyanurates is a singlet state which results from the shift of electron density from the periphery of the electron-rich branches toward the isocyanurate core (resembling a $E \leftarrow A$ transition under strict C_{3v} symmetry). Since the energy of this transition is directly connected to the HOMO-LUMO gap, it can be controlled by properly modifying the nature of the conjugated peripheral branches. Accordingly, either terminal substitution by electron-releasing substituents or lengthening of the π-manifold on these branches allows to red-shift this absorption band. In line with the octupolar symmetry of these derivatives, their GS is always nearly apolar, whereas their first excited state can be strongly polarized, especially for compounds featuring electron-releasing substituents at their periphery. In such instances, this excited state likely adopts a dipolar structure localized in one branch after vibrational relaxation, especially in highly polar media. Whether this solvent-dependent relaxation process implies also a concomitant change in electronic state (internal conversion) could not be presently established.

Also in relation to their octupolar structure, these compounds present remarkable third-order NLO properties. Thus, similar to what had previously been observed with **2-X** derivatives, their first excited state can be populated by two-photon excitation. The resulting 2PA cross-sections (Table 2) are strongly dependent upon the nature of the branches. Both the spatial elongation of the π-manifold of each branch and their polarization (*via* the terminal X substituents) will induce an increase of the 2PA cross-sections. In this respect, it has independently been established that the inclusion of electron-rich d^6 transition metal centers via alkynyl linkages constitutes an efficient alternative strategy for boosting the second- and third-order NLO properties of such carbon-rich structures.[24] For instance, cross-sections above 400 GM were found for the known isocyanurate derivatives **21** and **22** (Scheme 12).[13] However, the metal centers in these isocyanurates strongly quench the emission of the appended organic core[25] and **21** or **22** are essentially non-luminescent at ambient temperatures.[26] In contrast to these organometallic derivatives, the purely organic cyclotrimers presently reported are strongly fluorescent, allowing envisioning practical applications such as fluorescence imaging for these two-photon absorbers.

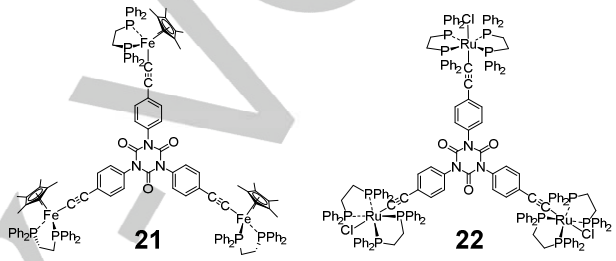

Scheme 12. Selected organometallic isocyanurates.

Two-photon brilliancy ($\Phi_F.\sigma_2$) is a crucial parameter for bio-imaging dyes,[27] but other important criteria are also to present an excitation wavelength well shifted in the near-IR region *i.e.* located in the optimal transparency window of the living tissues (650-900 nm) and to be vectorizable through aqueous media.[7b] A figure of merit allowing gauging the first property in function of the molecular size was considered (Table 4). Based on it, **4-NPh$_2$** and **14** appear as the best candidates among the new isocyanurates presently synthesized. For both molecules, two-photon excitation can be conveniently performed at 770 nm, which corresponds to population of the first excited state for the former compound and to population of a higher excited state for the second. When compared to the known **2-NPh$_2$** derivative, **4-NPh$_2$** appears slightly less promising based on this figure of merit, but its maximum absorbance is red-shifted by 40 nm, which can constitute an important advantage over **2-NPh$_2$** in case of transparency issues. By comparison, the derivative **14** has a much higher efficacy for molecular imaging according to both criteria. However, recalling that in order to be used for bio-imaging purposes, these molecules will need to be water-solubilized at some stage, analogues of **4-NPh$_2$** (or even of **2-NPh$_2$**) might also constitute good starting targets, given that derivatives such as **14** are currently much more challenging to synthesize.

Conclusions

During the course of this work, several new triaryl-isocyanurates were synthesized and characterized. The study of their optical properties indicates that inclusion of either 2,7-fluorenyl or 1,9-anthryl spacers at their periphery can give rise to chromophores more fluorescent and with higher 2PA cross-sections than the known **2-X** derivatives. Compared to compounds featuring exclusively 1,4-phenylene as aromatic units, the new derivatives present a first absorption and emission significantly red-shifted, well located in the transparency window of living tissues (*ca.* 650-900 nm), with higher molar absorption coefficients (especially in the case of fluorenyl derivatives), as well as presenting improved emission quantum yields. While these structural modifications induce less pronounced enhancements of the 2PA cross-sections than when d^6 transition-metal alkynyl endgroups were appended to the peripheral arms of triphenyl isocyanurate cores, we show that the fluorescence of the resulting organic derivatives is always preserved. Presently, the strong fluorescence of some of these dyes in solution and their good transparency in the visible range makes them better potential candidates for bioimaging applications than any isocyanurate derivative reported so far. Based on the available figures of merit, molecules such as **4-NPh$_2$** or **14** appear to constitute the best among them, provided they can be water-solubilized. In this respect, investigations aimed at developing more hydrophilic analogues of these molecules are now underway.

Experimental Section

General Procedures. All manipulations were carried out under an inert atmosphere of argon with dried and freshly distilled solvents (MeOH, distilled from Mg; THF, Et_2O and *n*-pentane, distilled from Na/benzophenone; CH_2Cl_2, distilled from CaH_2). The solvents used for spectroscopic measurements were of commercial origin: CH_3CN, MeOH, CH_2Cl_2, 1-BuOH, n-hexane and 1,4-dioxane from Merck (spectral grade), toluene from POCH (Poland, for analysis), 1-PrOH (Aldrich, spectrophotometric grade) and glycerol (99.5%, Sigma). Transmittance-FTIR spectra were recorded using a Perkin Elmer Spectrum 100 spectrometer equipped with a universal ATR sampling accessory (400-4000 cm^{-1}). Raman spectra of the solid samples were obtained by diffuse scattering on the same apparatus and recorded in the 100-3300 cm^{-1} range (Stokes emission) with a laser excitation source at 1064 nm (25 mW) or 633 nm (**14**) and a quartz separator with a FRA 106 detector. High field NMR spectra experiments were performed on multinuclear Bruker 200, 300 or 400 MHz instruments (200DPX, Avance 300 or Ascend400). Chemical shifts are given in parts per million relative to tetramethylsilane (TMS) for 1H and ^{13}C NMR spectra. UV-Visible spectra were recorded using a Cary 5000 spectrometer, a Jasco V-570 (solutions) or a Shimadzu UV 2700 double beam spectrophotometer. MS analyses were performed at the "Centre Regional de Mesures Physiques de l'Ouest" (CRMPO, University of Rennes) on a high resolution MS/MS ZABSpec TOF Micromass Spectrometer. Elemental analyses were also performed at the CRMPO. Commercial reagents were used as received. Tris(4-phenylethynyl)isocyanurate (**6**),[6a] 9,9-dibutyl-N,N-diphenyl-7-(iodo)-9H-fluoren-2-amine (**8**)[10] and 4-ethynyl-N,N-diphenylaniline[28] were synthesized as previously described by some of us, whereas compounds **7** and **9** have been recently independently reported, although they were obtained by a different synthetic route.[29]

1,3,5-tri(*9H*-fluoren-2-yl)-1,3,5-triazinane-2,4,6-trione (3). Under a stream of argon CsF (15 mg, 0.1 mmol) was added to a suspension of 2-fluorenyl isocyanate (1.0 g, 4.8 mmol) in degassed nitrobenzene (10 mL). The flask was sealed and the reaction mixture stirred at room temperature for 12 h. The cloudy solution was diluted with Et_2O (unless otherwise specified) and the precipitate collected. The solid was then washed repeatedly with Et_2O (3 x 20 mL), dried in vacuum and purified using column chromatography (Silica gel, eluting with dichloromethane) as an off-white solid. Yield: 530 mgs (53 %). **MP**: >266 °C. R_f: 0.32 (CH_2Cl_2/Heptane [8:2]). **HRMS**: (ESI): *m/z* = 644.1943 $[M+Na]^+$ (calc. for $C_{42}H_{27}N_3O_3Na$: 644.1945). **Anal.** Calc. for $C_{42}H_{27}N_3O_3$: C, 81.14, H, 4.38, N, 6.76; found: C, 80.86, H, 4.51, N, 6.74. **^{1}H NMR** (200 MHz, $CDCl_3$): δ = 7.95-7.90 (d, *J* = 8.2 Hz, 3H), 7.85-7.75 (m, 3H), 7.65-7.55 (m, 6H), 7.49-7.32 (m, 9H), 3.95 (s, 6H). **^{13}C{^{1}H}-NMR** (50 MHz, $CDCl_3$): δ = 149.6, 144.7, 144.0, 143.3, 141.0, 132.4, 127.8, 127.5, 127.4, 125.5, 120.9, 120.8, 37.3. **Anal.** Calc for $C_{42}H_{27}N_3O_3$: **IR** (KBr, cm^{-1}): $\bar{\upsilon}$ = 1771 (C=O, w), 1710 (C=O, vs). **Raman** (neat, cm^{-1}): $\bar{\upsilon}$ = 1771 (C=O, m).

Sonogashira Coupling Reaction; General Procedure

Method A

In an oven-dried Schlenk tube, to a mixture of **1-Br** (1 eq.), CuI (20 mol. %) and $PdCl_2(PPh_3)_2$ (10 mol. %) in DMF and Et_3N was added an excess of the alkyne (5 or 6 eq.). After 72 h of stirring at 70 °C and cooling to room temperature, the solvents were removed by cryoscopic transfer. The reaction mixture was extracted with CH_2Cl_2, washed with water and dried over $MgSO_4$. After filtration and evaporation to dryness, the crude product was purified by column chromatography on silica gel.

Method B

In an oven-dried Schlenk tube, to a mixture of **6**, CuI and $PdCl_2(PPh_3)_2$ in DMF and Et_3N was added an excess of the halogeno-chromophore (>3 eq.). After stirring at 70 °C for 72 h (unless otherwise indicated) and cooling to room temperature, the solvents were removed by cryoscopic transfer. The reaction mixture was extracted with CH_2Cl_2, washed with water and dried over $MgSO_4$. After filtration and evaporation to dryness, the crude product was purified by column chromatography on silica gel.

1,3,5-tris(4-(2-(9,9-dibutyl-*9H*-fluoren-2-yl)ethynyl)phenyl)-1,3,5-triazinane-2,4,6-trione (4-H). Following the general procedure (method B) with **6** (200 mg, 0.46 mmol), CuI (6 mg, *ca.* 8% mol), $PdCl_2(PPh_3)_2$ (11 mgs, *ca.* 4% mol), DMF (30 mL), Et_3N (10 mL), and commercial 2-bromo-9,9-dibutyl-*9H*-fluorene (530 mg, 1.48 mmol; 3.2 eq.) were reacted. After removal of the solvents, the crude solid was purified by column chromatography with hexane/Et_2O (1:1) and the title compound was isolated as a yellow solid. Yield: 350 mg (60 %). **MP**: 148-140 °C (Dec). R_f: 0.47 (hexane/Et_2O [1:1]). **HRMS**: (ESI): *m/z* = 1280.6628 $[M+Na]^+$ (calc. for $C_{90}H_{87}N_3O_3Na$: 1280.6640). **^{1}H NMR** (200 MHz, CD_2Cl_2): δ = 7.77-7.69 (m, 12H, H_{Ar}), 7.59-7.53 (m, 6H, H_{Ar}), 7.50-7.30 (m, 15H, H_{Flu}), 2.02 (m, 12H, $CH_{2/Bu}$), 1.09 (m, 12H, $CH_{2/Bu}$), 0.75-0.50 (m, 30H, $CH_{3/Bu}$ + $CH_{2/Bu}$). **^{13}C{^{1}H} NMR** (50 MHz, $CDCl_3$): δ = 151.7, 151.4, 148.4, 140.9, 133.5, 133.4, 133.1, 131.4, 129.2, 128.3, 127.5, 126.7, 125.6, 123.5, 121.5, 120.7, 120.3, 92.8, 88.9, 55.7, 40.8, 26.5, 23.7, 14.5. **IR** (KBr, cm^{-1}): $\bar{\upsilon}$ = 2203 (C≡C, w), 1777 (C=O, vw), 1720 (C=O, vs). **Raman** (neat, cm^{-1}): $\bar{\upsilon}$ = 2206 (C≡C, s), 1781 (C=O, vw).

1,3,5-tris(4-(2-(9,9-dibutyl-2-(diphenylamino)-9H-fluoren-7-yl)ethynyl)phenyl)-1,3,5-triazinane-2,4,6-trione (4-NPh$_2$). Following the general procedure (method A) with **1-Br** (101 mg, 0.17 mmol), CuI (6.5 mg, 0.034 mmol), $PdCl_2(PPh_3)_2$ (12 mg, 0.017 mmol), DMF (50 mL), Et_3N (10 mL), and (9,9-dibutyl-7-ethynyl-9H-fluoren-2-yl)-diphenyl-amine (**7**; 400 mg,

0.85 mmol). The crude material was purified by column chromatography with AcOEt/Hexane (4/1) to afford the title product as a yellow-orange solid. Yield: 280 mg (93 %). **MP**: 154-148 °C (Dec). R_f: 0.29 (Ethyl Acetate/Hexane [1:17]) **HRMS**: (ESI): *m/z* = 1781.8856 $[M+Na]^+$ (calc. for $C_{126}H_{114}N_6O_3Na$: 1781.8850). **^{1}H NMR** (300 MHz, $CDCl_3$): δ = 7.71 (d, 6H, *J* = 8.4 Hz), 7.63-7.49 (m, 12H), 7.44 (d, 6H, *J* = 8.4 Hz), 7.29 (m, 12H), 7.16 (m, 15H), 7.06 (m, 9H), 1.89 (m, 12H), 1.10 (m,12H), 0.77-0.55 (m, 30H, overlapped). **^{13}C{^{1}H} NMR** (101 MHz, $CDCl_3$): δ = 153.1, 151.3, 148.9, 148.5, 148.3, 142.3, 135.9, 133.6, 131.5, 129.8, 129.2, 126.5, 125.7, 124.6, 123.9, 123.3, 121.5, 120.6, 119.7, 119.6, 93.0, 88.8, 55.7, 40.6, 26.6, 23.6, 14.5. **IR** (KBr, cm^{-1}): $\bar{\upsilon}$ = 2198 (C≡C, vw), 1778 (C=O, w), 1720 (C=O, vs). **Raman** (neat, cm^{-1}): $\bar{\upsilon}$ = 2206 (C≡C, m), 1778 (C=O, vw).

1,3,5-tris(4-(2-(10-((2-methoxyethoxy)methyl)anthracen-9-yl)ethynyl) phenyl)-1,3,5-triazinane-2,4,6-trione (5-MEM). Following the general procedure (method A) with **1-Br** (238 mg, 0.4 mmol), CuI (15.2 mg, 0.08 mmol), $PdCl_2(PPh_3)_2$ (28 mgs, 0.04 mmol), DMF (50 mL), Et_3N (10 mL), and 9-Ethynyl-10-(2-methoxy-ethoxymethyl)anthracene (**10**; 590 mg, 2.03 mmol). The crude solid was purified by column chromatography with AcOEt/hexane (from 50/50 to 100/0) to afford the title product as a yellow-orange solid. Yield: 440 mg (90 %). **MP**: >260 °C. R_f: 0.62 (CH_2Cl_2/Ethyl Acetate [19:1]). **HRMS**: (ESI): *m/z* = 1244.4454 $[M+Na]^+$ (calc. for $C_{81}H_{63}N_3O_9Na$: 1244.4456). **Anal.** Calc. for $C_{81}H_{63}N_3O_9$: C, 79.59, H, 5.19, N, 3.44; found: C, 78.10, H, 5.19, N, 3.28. **^{1}H NMR** (300 MHz, $CDCl_3$): δ = 8.70 (d, 6H, *J* = 9.0 Hz), 8.48 (d, 6H, *J* = 9.0 Hz), 7.93 (d, 6H, *J* = 9.0 Hz), 7.61 (m, 18H), 5.57 (s, 6H), 3.79 (m, 6H), 3.58 (m, 6H), 3.39 (s, 9H). **^{13}C{^{1}H} NMR** (101 MHz, CD_2Cl_2): δ = 148.7, 134.1, 133.0, 132.8, 131.5, 130.9, 129.3, 127.6, 126.9, 126.8, 125.4, 125.3, 118.5, 100.5, 88.4, 72.6, 70.3, 65.6, 59.1. **IR** (KBr, cm^{-1}): $\bar{\upsilon}$ = 2192 (C≡C, w), 1772 (C=O, vw), 1713 (C=O, s), 1092, (C-O, m). **Raman** (neat, cm^{-1}): $\bar{\upsilon}$ = 2197 (C≡C, vs), 1771 (C=O, w).

9,9-di-*n*-butyl-N,N-diphenyl-7-ethynyl-9H-fluoren-2-amine (7). 9,9-di-*n*-butyl-N,N-diphenyl-7-((trimethylsilyl)ethynyl)-9H-fluoren-2-amine (**9**; 0.642 g, 1.2 mmol) was dissolved in THF (15 mL), then tetrabutylammonium fluoride 1.0 M solution in THF (1.2 mL, 1.2 mmol) was slowly syringed in the medium (dropwise) and the reaction medium was stirred at 20 °C for 2 h. The reaction mixture was extracted with Et_2O, washed with water, dried on $MgSO_4$ and evaporated to dryness to afford a pale yellow amorphous solid which was subsequently engaged in the next step. Yield: 0.54 g (96 %). **MP**: 48-55 °C (Dec). R_f: 0.26 (CH_2Cl_2/Hexane [1:9]). **^{1}H NMR** (400 MHz, $CDCl_3$): δ = 7.60 (d, *J* = 8.1 Hz, 2H), 7.55-7.49 (m, 2H), 7.31 (t, *J* = 7.8 Hz, 4H), 7.21 (d, *J* = 7.0 Hz, 5H), 7.14-7.04 (m, 3H), 3.16 (s, 1H), 2.03-1.84 (m, 4H), 1.26-1.06 (m, 4H), 0.86-0.64 (m, 10H). **^{13}C{^{1}H} NMR** (101 MHz, $CDCl_3$): δ = 153.2, 151.3, 148.8, 148.6, 142.7, 135.9, 131.9, 129.9, 127.1, 124.7, 123.9, 123.4, 121.4, 119.9, 119.6, 85.6, 55.7, 40.6, 26.7, 23.7, 14.5. **IR** (KBr, cm^{-1}): $\bar{\upsilon}$ = 3284 (≡C-H, m), 2102 (C≡C, w). **Raman** (neat, cm^{-1}): $\bar{\upsilon}$ = 2102 (C≡C, s).

9,9-di-*n*-butyl-N,N-diphenyl-7-((trimethylsilyl)ethynyl)-9H-fluoren-2-amine (9). 2-diphenylamino-5-iodo-*9,9*-di-*n*-butyl-fluorene (**8**; 1.43 g, 2.5 mmol), CuI (11.5 mg, 0.06 mmol), $PdCl_2(PPh_3)_2$ (37.9 mg, 0.05 mmol) and 2-(trimethylsilyl)acetylene (0.55 mL, 3.9 mmol) were introduced in a Schlenk flask under argon and freshly degazed Et_3N (10 mL) was added. The heating to 40°C was started and the reaction medium was left stirring for 13 h. After cooling to room temperature, the reaction mixture was filtrated on silica, washed with CH_2Cl_2 and evaporated to dryness. The resulting solid was subsequently purified by column chromatography with CH_2Cl_2/heptane (from 0/10 to 2/8) followed by a precipitation in heptane to afford the title product as a pale yellow solid. Yield: 0.84 g (62 %). **MP**: 164 °C (Dec). R_f: 0.22 (CH_2Cl_2/Hexane [1:9]). **HRMS** (ESI): *m/z* = 564.3061 $[M+Na]^+$ (calc. for $C_{38}H_{43}NNaSi$: 564.3062). **^{1}H NMR** (300 MHz, $CDCl_3$): δ = 7.54 (d, J = 8.2 Hz, 2H), 7.49-7.37 (m, 2H), 7.27-7.20 (m, 4H), 7.18-7.08 (m, 5H), 7.08-6.99 (m, 3H), 1.96-1.75 (m, 4H), 1.18-0.99 (m, 4H), 0.78 – 0.50 (m, 10H), 0.30 (s, 9H). **^{13}C{^{1}H} NMR** (75 MHz, $CDCl_3$): δ = 152.5, 150.5, 147.9, 147.7, 141.5, 135.4, 131.3, 129.2, 126.1, 124.0, 123.3, 122.7, 120.7, 120.4, 119.0, 118.9, 106.5, 93.6, 55.0, 40.0, 26.0, 23.0, 13.9, 0.1. **IR** (KBr, cm^{-1}): $\bar{\upsilon}$ = 2154 (C≡C, vw).

10-((2-methoxyethoxy)methyl)-9-ethynylanthracene (10). In an oven-dried Schlenk tube, 10-((2-methoxyethoxy)methyl)-9-(2,2-dibromovinyl)-anthracene (**12**) (2 g, 4.44 mmol) was dissolved in THF (20 mL), and the mixture was cooled down to -90 °C, before adding LDA (6.7 mL, 13.3 mmol, 2 M in THF-heptane, 3 eq.). After stirring at -90 °C for 1.5 h, the reaction mixture was allowed to warm at 25 °C and then, was hydrolyzed (0 °C), extracted with CH_2Cl_2 and washed with water and dried over $MgSO_4$. After filtration and evaporation to dryness, the crude solid was adsorbed on SiO_2 and purified by column chromatography on silica gel with AcOEt/Hexane (1:4) to afford the title product as a yellow-orange solid. Yield: 750 mg (58 %). **MP**: 66 °C (Dec). R_f: 0.14 (CH_2Cl_2/Heptane [1:1]). **HRMS** (ESI): *m/z* = 313.1207 $[M+Na]^+$ (calc. for $C_{20}H_{18}O_2Na$: 313.1205). **Anal.** Calc. for $C_{20}H_{18}O_2$: C, 82.73, H, 6.25; found: C, 82.92, H, 6.27. **^{1}H NMR** (400 MHz, $CDCl_3$): δ = 8.71-8.58 (m, 2H), 8.53-8.41 (m, 2H), 7.64-7.51 (m, 4H), 5.56 (s, 2H), 4.02 (s, 1H), 3.83-3.71 (m, 2H), 3.62-3.49 (m, 2H), 3.39 (s, 3H). **^{13}C{^{1}H} NMR** (101 MHz, $CDCl_3$): δ = 133.0, 130.8, 130.7, 127.4, 126.5, 126.5, 125.0, 117.9, 89.0, 80.6, 72.4, 69.6, 65.4, 59.2. **IR** (KBr, cm^{-1}): $\bar{\upsilon}$ = 3230 (≡C-H, s), 2055 (C≡C, vw).

9-((2-methoxyethoxy)methyl)anthracene-10-carbaldehyde (11). In an oven-dried Schlenk tube, was dissolved 9,10-dibromoanthracene (4.40 g, 13.1 mmol, 1 eq.) in THF (100 mL). After cooling it to -90 °C, *n*-BuLi (1.6 M in THF solution, 9 mL, 1.1 eq.) was slowly added and the mixture was allowed to stir for 30 mn, then 1-(chloromethoxy)-2-methoxyethane (1.65 mL, 1.1 eq.) was also added and the mixture allowed to stir for 10 additionnal mn. After heating up at 0 °C, a second equivalent of *n*-BuLi was added following the same procedure, followed by the addition of DMF (3 mL, 3 eq.). After stirring at room temperature overnight, the reaction mixture was hydrolyzed, extracted with CH_2Cl_2, washed with water and dried over $MgSO_4$. After filtration and evaporation to dryness, the crude solid was adsorbed on SiO_2 and purified by column chromatography on silica gel with AcOEt/Hexane (1:2) to afford the title product as a pale yellow solid. Yield: 1.89 g (49 %). **MP**: 74 °C (Dec). R_f: 0.32 (AcOEt/Petroleum ether [1:2]). **HRMS** (ESI): *m/z* = 317.1154 $[M+Na]^+$ (calc. for $C_{19}H_{18}O_3Na$: 317.1153). **Anal.** Calc. for $C_{19}H_{18}O_3$: C, 77.53, H, 6.16; found: C, 77.14, H, 6.33. **^{1}H NMR** (300 MHz, $CDCl_3$): δ = 11.36 (s, 1H), 8.85-8.69 (m, 2H), 8.50-8.34 (m, 2H), 7.64-7.51 (m, 4H), 5.41 (s, 2H), 3.85-3.66 (m, 2H), 3.61-3.50 (m, 2H), 3.39 (s, 3H).**^{13}C{^{1}H} NMR** (101 MHz, $CDCl_3$): δ = 194.0, 136.8, 131.4, 130.7, 128.4, 127.0, 126.4, 125.4, 124.1, 72.4, 70.0, 65.6, 59.3. **IR** (KBr, cm^{-1}): $\bar{\upsilon}$ = 1669 (C=O, vs).

10-((2-methoxyethoxy)methyl)-9-(2,2-dibromovinyl)anthracene (12). In an oven-dried Schlenk tube, was dissolved triphenylphosphine (4.21 g, 16 mmol, 2.5 eq.) in CH_2Cl_2 (30 mL). After cooling it to -20 °C, CBr_4 (5.33 g, 16 mmol, 2.5 eq.) was added and the mixture was allowed to stir for 1 h. Then, after cooling it to -70 °C, 9-((2-methoxyethoxy)methyl)-anthracene-10-carbaldehyde (**11**; 1.8 g, 6.1 mmol, 1 eq) and NEt_3 (1.42 mL, 1.6 eq.) in CH_2Cl_2 (30 mL) was added and the resulting mixture allowed to warm at 25 °C and stirred during 15 h. Then, the reaction was hydrolyzed, extracted with CH_2Cl_2, washed with water and dried over $MgSO_4$. After filtration and evaporation to dryness, the crude solid was adsorbed on SiO_2 and purified by column chromatography on silica gel with AcOEt/Hexane (1:2) to afford the title product as an amber solid. Yield: 2.33 g (85 %). **MP**: 88 °C (Dec). R_f: 0.44 (AcOEt/Petroleum ether [1:2]). **HRMS** (ESI): *m/z* = 470.9547 $[M+Na]^+$ (calc. for $C_{20}H_{18}Br_2O_2Na$: 470.9541). **Anal.** Calc. for $C_{20}H_{18}Br_2O_2$: C, 53.36, H, 4.03; found: C, 52.86, H, 3.97. **^{1}H NMR** (400 MHz, $CDCl_3$): δ = 8.50 (dd, *J* = 8.5, 1.8 Hz,

2H), 8.16 – 8.04 (m, 3H), 7.69-7.52 (m, 4H), 5.58 (s, 2H), 3.88-3.78 (m, 2H), 3.67-3.57 (m, 2H), 3.42 (s, 3H). **$^{13}C\{^1H\}$ NMR** (101 MHz, $CDCl_3$): δ = 135.9, 131.9, 130.9, 130.2, 128.5, 126.4, 126.1, 126.0, 125.1, 95.6, 72.4, 69.8, 65.6, 59.2. **IR** (KBr, cm^{-1}): $\bar{\upsilon}$ = 1590 (C=C, w).

1,3,5-tris(4-((9,9-di-*n*-butyl-7-((4-(diphenylamino)phenyl)ethynyl)-9H-fluoren-2-yl)ethynyl)phenyl)-1,3,5-triazinane-2,4,6-trione (13). Following the general procedure (method B) with **6** (0.069 g, 0.16 mmol, 1 eq.), CuI (6 mg, 0.03 mmol), $PdCl_2(PPh_3)_2$ (11 mg, 0.016 mmol) and 4-((9,9-di-*n*-butyl-2-(2-iodo-9H-fluoren-7-yl)ethynyl)phenyl)-N-phenylbenzenamine (**15**; 0.433 g, 0.64 mmol), DMF (50 mL) and Et_3N (15 mL). The crude solid was purified by column chromatography with CH_2Cl_2/Hexane (3:2), followed by a second separation on preparative plate (Eluent: CH_2Cl_2/Hexane [8:7]) to afford the title product as a pale orange solid. Yield: 35 mg (10 %). **MP**: 168 °C. ***R*f**: 0.51 (CH_2Cl_2/Hexane [3:2]). **HRMS** (ESI): *m/z* = 1029.4928 $[M]^{++}$ (calc. for $C_{150}H_{126}N_6O_3$: 1029.4940), 2058.9815 $[M]^+$ (calc. for $C_{150}H_{126}N_6O_3$: 2058,9886). **^1H NMR** (300 MHz, CD_2Cl_2): δ = 7.80-7.67 (m, 12H), 7.65-7.25 (m, 24H), 7.20-6.90 (m, 36H), 2.06 (m, 12H), 1.16 (m, *J* = 6 Hz, 12H), 0.75 (t, *J* = 6 Hz, 18H), 0.62 (m, 12H). **$^{13}C\{^1H\}$ NMR** (101 MHz, CD_2Cl_2): δ = 151.6, 151.6, 148.7, 148.4, 147.6, 141.6, 140.7, 133.7, 132.8, 132.7, 131.2, 130.9, 129.8, 129.1, 126.6, 126.2, 125.5, 125.3, 124.3, 124.1, 122.9, 122.4, 120.4, 120.3, 116.3, 92.4, 90.5, 89.8, 88.7, 55.6, 40.5, 26.4, 23.4, 14.0. **IR** (KBr, cm^{-1}): $\bar{\upsilon}$ = 2195 (C≡C, w), 1778 (C=O, vw), 1717 (C=O, vs). **Raman** (neat, cm^{-1}): $\bar{\upsilon}$ = 2201 (C≡C, w), 1780 (C=O, vw).

1,3,5-tris(4-((10-((4-(diphenylamino)phenyl)ethynyl)anthracen-9-yl)-ethynyl)phenyl)-1,3,5-triazinane-2,4,6-trione (14). Following the general procedure (method A) with **1-Br** (0.125 g, 0.21 mmol, 1 eq.), CuI (8 mg, 0.04 mmol), $PdCl_2(PPh_3)_2$ (15 mg, 0.02 mmol) and 4-((10-ethynylanthracen-9-yl)ethynyl)-N,N-diphenylaniline (**16**; 0.406 g, 0.86 mmol, 4 eq.) in DMF (50 mL) and NEt_3 (20 mL). Purified by column chromatography with AcOEt/Hexane (from 1:3 to 100:0), the title product was isolated admixed with traces of **19** and **20** (MS evidence). After adsorption of this fraction on silica gel and after performing a second chromatographic separation of this absorbate using a CH_2Cl_2/petroleum ether gradient, the title product was isolated as an orange solid. Yield: 33 mg (8 %). **MP**: >260 °C (Dec). ***R*f**: 0.29 (CH_2Cl_2/Petroleum ether [6:4]). **HRMS** (ESI): *m/z* = 879.3056 $[M]^{++}$ (calc. for $C_{129}H_{78}N_6O_3$: 879.3062), 1758.6094 $[M]^+$ (calc. for $C_{129}H_{78}N_6O_3$: 1758,6130). **^1H NMR** (300 MHz, $CDCl_3$): δ = 8.82-8.65 (m, 12H), 7.96 (d, *J* = 8.6 Hz, 6H), 7.76-7.61 (m, 18H), 7.57 (d, *J* = 8.6 Hz, 6H), 7.41-7.30 (m, 12H), 7.23-7.08 (m, 24H). **$^{13}C\{^1H\}$ NMR** (75 MHz, $CDCl_3$): δ = 148.4, 148.3, 147.1, 133.3, 132.7, 132.6, 132.3, 131.9, 129.5, 128.8, 127.4, 127.1, 127.0, 126.7, 125.2, 124.1, 123.8, 122.3, 119.6, 117.2, 116.0, 103.4, 100.9, 88.3, 85.9. **IR** (KBr, cm^{-1}): $\bar{\upsilon}$ = 2183 (C≡C, broad w), 1772 (C=O, vw), 1720 (C=O, s). **Raman** (neat, cm^{-1}): $\bar{\upsilon}$ = 2183 (C≡C, w).

N-(4-(2-(9,9-di-*n*-butyl-2-(2-iodo-9H-fluoren-7-yl)ethynyl)phenyl)-N-phenylbenzenamine (15). 2,7-diodo-9,9-di-*n*-butyl-fluorene (2.07 g, 3.9 mmol), CuI (11.9 mg, 0.08 mmol), $PdCl_2(PPh_3)_2$ (36 mg, 0.04 mmol) and 4-(2-(trimethylsilyl)ethynyl)diphenylaniline (0.84 g, 2.46 mmol) were introduced in a Schlenk flask under argon and freshly degazed Et_3N (5 mL) was added. The heating to 40 °C was started, a TBAF 1.0 M solution in THF (2.70 mL, 2.70 mmol) was then slowly syringed in the medium (dropwise) and the reaction medium was left stirring for 27 h. After cooling to room temperature, the solvents were removed by evaporation. The reaction mixture was extracted with CH_2Cl_2, washed with water, filtrated on silica and evaporated to dryness. The resulting solid was subsequently purified by column chromatography with CH_2Cl_2/heptane (from 1/9 to 2/8) to afford the title product as a yellow solid. Yield: 0.76 g (46 %). **MP**: 162 °C (Dec). ***R*f**: 0.35 (CH_2Cl_2/Hexane [1:1]). **HRMS** (ESI): *m/z* = 694.1943 $[M+Na]^+$ (calc. for $C_{41}H_{38}NINa$: 694.1941). **^1H NMR** (300 MHz, $CDCl_3$): δ = 7.71-7.61 (m, 3H), 7.54-7.39 (m, 5H), 7.35-7.27 (m, 4H), 7.19-7.01 (m, 8H), 2.06-1.86 (m, 4H), 1.11 (hept, *J* = 7.4 Hz, 4H), 0.71 (t, *J* = 7.3 Hz, 6H), 0.66-0.53 (m, 4H). **$^{13}C\{^1H\}$ NMR** (75 MHz, $CDCl_3$): δ = 153.4, 150.2, 147.9, 147.2, 140.2, 140.0, 136.0, 132.5, 132.1, 130.6, 129.4, 125.7, 125.0, 123.6, 122.5, 122.3, 121.6, 119.8, 116.0, 93.0, 90.1, 89.6, 55.3, 40.1, 25.9, 23.0, 13.8. **IR** (KBr, cm^{-1}): $\bar{\upsilon}$ = 2202 (C≡C, w).

4-((10-ethynylanthracen-9-yl)ethynyl)-N,N-diphenylaniline (16). In an oven-dried Schlenk tube, 4-((10-(2,2-dibromovinyl)anthracen-9-yl)ethynyl)-N,N-diphenylaniline (**18**; 1.09 g, 1.73 mmol) was dissolved in THF (20 mL), and the mixture was cooled down to -90 °C, before adding LDA 2.0 M in THF-heptane (1.8 mL, 3.6 mmol). After stirring at -90 °C for 1.5 h, the reaction mixture was allowed to warm at 25 °C and then, was hydrolyzed (0 °C), extracted with CH_2Cl_2 and washed with water and dried over $MgSO_4$. After filtration and evaporation to dryness, the crude solid was adsorbed on SiO_2 and purified by column chromatography on silica gel with CH_2Cl_2/Hexane (1:1) to afford the title product as an intense red solid. Yield: 540 mg (66 %). **MP**: 224 °C (Dec). ***R*f**: 0.63 (CH_2Cl_2/Petroleum ether [1:1]). **HRMS** (ESI): *m/z* = 492.1723 $[M+Na]^+$ (calc. for $C_{36}H_{23}N_1Na_1$: 492.1722). **^1H NMR** (300 MHz, CD_2Cl_2): δ = 8.79-8.53 (m, 4H), 7.73-7.53 (m, 6H), 7.41-7.26 (m, 4H), 7.23-7.02 (m, 8H), 4.16 (s, 1H). **$^{13}C\{^1H\}$ NMR** (100 MHz, CD_2Cl_2): δ = 149.2, 147.6, 133.2, 132.2, 130.1, 127.8, 127.7, 127.4, 127.3, 125.9, 124.5, 122.4, 120.2, 117.0, 116.1, 104.0, 90.4, 86.0, 80.8. **IR** (KBr, cm^{-1}): $\bar{\upsilon}$ = 3290 (≡C-H, m), 2182 (C≡C, m), 2091 (C≡CH, w).

10-((4-(diphenylamino)phenyl)ethynyl)anthracene-9-carbaldehyde (17). In an oven-dried Schlenk tube, 10-bromoanthracene-9-carbaldehyde (2.42 g, 7.5 mmol, 1 eq.), CuI (114 mg, 0.60 mmol), $PdCl_2(PPh_3)_2$ (210 mg, 0.29 mmol) and 9- 4-ethynyl-*N,N*-diphenylaniline (2.75 g, 10.2 mmol) were dissolved in THF (40 mL) under argon. Subsequently, 30 mL of degassed NEt_3 were added and the reaction medium was stirred 14 h at 70 °C. The solvents were then removed by cryoscopic transfer and the reaction mixture was extracted with CH_2Cl_2, washed with water and dried over $MgSO_4$. After filtration and evaporation to dryness, the crude solid was purified by column chromatography with CH_2Cl_2/Hexane (1:1) to afford the title product as an orange solid. Yield: 3.16 g (89 %). **MP**: 260 °C (Dec). ***R*f**: 0.25 (CH_2Cl_2/Petroleum ether [1:1]). **HRMS** (ESI): *m/z* = 496.1672 $[M+Na]^+$ (calc. for $C_{35}H_{23}N_1Na_1O_1$: 496.1677). **Anal.** Calc. for $C_{35}H_{23}NO$: C, 88.77, H, 4.90, N, 2.96; found: C, 87.07, H, 4.98, N, 2.86. **^1H NMR** (300 MHz, CD_2Cl_2): δ = 11.49 (s, 1H), 9.02-8.90 (m, 2H), 8.85-8.74 (m, 2H), 7.77-7.58 (m, 6H), 7.42-7.28 (m, 4H), 7.23-7.04 (m, 8H). **$^{13}C\{^1H\}$ NMR** (75 MHz, CD_2Cl_2): δ = 193.4, 149.6, 147.5, 133.4, 132.1, 131.9, 130.1, 129.5, 128.3, 127.1, 126.6, 126.0, 125.2, 124.7, 124.4, 122.1, 115.3, 106.4, 86.2. **IR** (KBr, cm^{-1}): $\bar{\upsilon}$ = 2190 (C≡C, m), 1671 (C=O, vs).

4-((10-(2,2-dibromovinyl)anthracen-9-yl)ethynyl)-N,N-diphenylaniline (18). In an oven-dried Schlenk tube, was dissolved triphenylphosphine (2.76 g, 10.5 mmol) in CH_2Cl_2 (30 mL). After cooling it to -20 °C, CBr_4 (3.5 g, 10.5 mmol) was added and the mixture was allowed to stir for 1 h. Then, after cooling it to -70 °C, a mixture of 10-((4-(diphenylamino)-phenyl)ethynyl)anthracene-9-carbaldehyde (**17**; 2.0 g, 4.22 mmol) and NEt_3 (0.95 mL, 6.75 mmol) in CH_2Cl_2 (30 mL) was added. The resulting mixture was allowed to warm at 25 °C and stirred 15 h. Then, the reaction mixture was hydrolyzed, extracted with CH_2Cl_2, washed with water and dried over $MgSO_4$. After filtration and evaporation to dryness, the crude solid was adsorbed on SiO_2 and purified by column chromatography on silica gel with CH_2Cl_2/Hexane (1:1) to afford the title product as a yellow solid. Yield: 1.34 g (50 %). **MP**: 242 °C (Dec). ***R*f**: 0.65 (CH_2Cl_2/Hexane [1:1]). **HRMS** (ESI): *m/z* = 627.0200 $[M]^+$ (calc. for $C_{36}H_{23}Br_2N_1$: 627.0197). **Anal.** Calc. for $C_{36}H_{23}Br_2N_1$: C, 68.70, H, 3.68, N, 2.23; found: C, 68.96, H, 3.68, N, 2.25. **^1H NMR** (300 MHz, CD_2Cl_2): δ = 8.76-8.67 (m, 2H), 8.16 (s, 1H), 8.14-8.07 (m, 2H), 7.67-7.57 (m, 6H),

7.38-7.28 (m, 4H), 7.21-7.04 (m, 8H). **$^{13}C\{^{1}H\}$ NMR** (75 MHz, CD_2Cl_2): δ = 149.1, 147.6, 136.1, 133.1, 132.5, 131.4, 130.0, 128.9, 127.9, 127.2, 127.1, 126.4, 125.8, 124.4, 122.5, 119.7, 116.3, 103.0, 96.2, 85.9. **IR** (KBr, cm^{-1}): $\bar{\upsilon}$ = 2190 (C≡C, m), 1586 (C=C, w).

Fluorescence measurements. The samples used to make the solutions were freshly recrystallized or thoroughly washed with cooled ether / pentane to remove any organic impurity prior to the measurements. Fluorescence measurements in solution were performed in dilute air-equilibrated solutions contained in quartz cells of 1 cm path length (*ca.* 10^{-6} M, optical density < 0.1) at room temperature (20 °C), using an Edinburgh Instruments (FLS920) spectrometer in photon-counting mode. Fully corrected excitation and emission spectra were obtained with an optical density at $\lambda_{exc} \leq 0.1$. Fluorescence quantum yields were measured according to literature procedures.[30] UV-vis absorption spectra used for the calculation of the fluorescence quantum yields were recorded using a double beam Jasco V-570 spectrometer.

Fluorescence Anisotropy Measurements. All the measurements were done using 10x10 mm path length Spectrosil quartz cuvettes (Starna). Steady state fluorescence emission spectra and anisotropy were recorded on an FS5 spectrofluorometer (Edinburgh Instruments), equipped with polarizers. The fluorescence quantum yield was measured using a standard comparative method using quinine sulfate in 0.05 M sulfuric acid solution in water (Φ_F = 0.52) or Coumarin 153 in ethanol solution (Φ_F = 0.58) as standards. Fluorescence lifetimes were measured on a homebuilt spectrometer, described in detail elsewhere.[31]

Two-photon excited fluorescence measurements. 2PA cross-sections (σ_2) were derived from the two-photon excited fluorescence (2PEF) cross-sections ($\sigma_2\Phi_F$) and the fluorescence emission quantum yield (Φ_F). 2PEF cross sections were measured relative to fluorescein in 0.01 M aqueous NaOH[32] using the well-established method described by Xu and Webb[33] and the appropriate solvent-related refractive index corrections.[34] Reference values between 700 and 715 nm for fluorescein were taken from literature.[35] The quadratic dependence of the fluorescence intensity on the excitation power was checked for each sample and all wavelengths. Measurements were conducted using an excitation source delivering fs pulses. A Chameleon Ultra II (Coherent) was used generating 140 fs pulses at 80 MHz repetition rate. The excitation was focused into the cuvette through a microscope objective (10X, NA 0.25). The fluorescence was detected in epifluorescence mode via a dichroic mirror (Chroma 675dcxru) and a barrier filter (Chroma e650sp-2p) by a compact CCD spectrometer module BWTek BTC112E. Total fluorescence intensities were obtained by integrating the corrected emission.

Z-scan studies: The measurements of the third-order nonlinear optical properties were carried out using the standard Z-scan technique with amplified femtosecond laser system using a Clark-MXR CPA-2001 Ti-sapphire regenerative amplifier to pump a Light Conversion TOPAS optical parametric amplifier. The pulse duration was approximately 150 fs and the repetition rate was 250 Hz. The pulse energy was adjusted to keep the nonlinear phase shifts that were obtained from the samples in the range of roughly 0.3–0.8 rad, light intensities ~60 GW/cm^2. Results obtained for samples in dichloromethane solutions placed in 1 mm stoppered Starna glass cells were calibrated against Z-scan measurements on a fused silica plate and compared with the measurements on an identical glass cell filled with the pure solvent.[36] The obtained data were analysed with the help of a custom fitting program that used equations derived by Sheik-Bahae *et al*.[37]

Computational Details. The DFT calculations reported in this work have been performed using the Gaussian09 [38] program. The geometries of all the compounds have been optimized without symmetry constraints using the MPW1PW91 functional[39] and the 6-31G* basis set. The solvent effects were taken into account by the means of the Polarizable Continuum Model (PCM).[40] The calculation of the frequencies of normal modes of vibration have then been carried out to confirm the true minima character of optimized geometries. Next, TD-DFT calculations have been performed at the same level of theory using the previously optimized geometries. In addition, Swizard[41] is used for plotting the simulated spectra, and GausView[42] for the MO plots.

Acknowledgements

The ANR (ANR-17-CE07-0033-01 project), the Erasmus program and Campus France (PHC Polonium Program 2017 N°37629XG) are acknowledged for financial support. Financial support from National Science Centre (Poland) under Harmonia project - UMO-2016/22/M/ST4/00275 grants is acknowledged. FP and FM acknowledge F. Audren (ISCR) for experimental support. We also acknowledge the HPC resources of CINES and of IDRIS under the allocations 2017-[x2015080649] and 2018-[x2016080649] made by GENCI (Grand Equipement National de Calcul Intensif).

Keywords: Anisotropy • Fluorescence • Isocyanurates • Nonlinear optics • Two-photon absorption.

[1] A. W. Hofmann, *Chem. Ber.* **1870**, *3*, 761-772.

[2] a) R. P. Tiger, L. I. Sarynina, S. G. Entelis, *Russ. Chem. Rev.* 1985, 41, 774. b) F. Paul, S. Moulin, O. Piechaczyk, P. Le Floch, J. A. Osborn, *J. Am. Chem. Soc.* **2007**, *129*, 7294-7304.

[3] D. K. Hoffmann, *J. Cell. Plast.* **1984**, *20*, 129-137.

[4] a) J. Zyss, I. Ledoux, *Chem. Rev.* 1994, 94, 77-105. b) W. H. Lee, S. H. Lee, J.-A. Kim, J. H. Choi, M. Cho, S.-J. Jeon, B. R. Cho, *J. Am. Chem. Soc.* **2001**, *123*, 10658-10667.

[5] V. R. Thalladi, S. Brasselet, D. Bläser, R. Boese, J. Zyss, A. Nangia, G. R. Desiraju, *Chem. Commun.* **1997**, 1841-1842.

[6] a) G. Argouarch, R. Veillard, T. Roisnel, A. Amar, H. Meghezzi, A. Boucekkine, V. Hugues, O. Mongin, M. Blanchard-Desce, F. Paul, *Chem. Eur. J.* **2012**, *18*, 11811-11826. b) G. Argouarch, R. Veillard, T. Roisnel, A. Amar, A. Boucekkine, A. Singh, I. Ledoux, F. Paul, *New J. Chem.* **2011**, *35*, 2409-2411.

[7] a) G. S. He, L.-S. Tan, Q. Zheng, P. N. Prasad, *Chem. Rev.* **2008**, *108*, 1245-1330. b) M. Pawlicki, H. A. Collins, R. G. Denning, H. L. Anderson, *Angew. Chem. Int. Ed.* **2009**, *48*, 3244-3266.

[8] a) O. Mongin, L. Porrès, M. Charlot, C. Katan, M. Blanchard-Desce, *Chem. Eur. J.* **2007**, *13*, 1481-1498. b) K. D. Belfield, A. R. Morales, B.-S. Kang, J. M. Hales, D. J. Hagan, E. W. van Stryland, V. M. Chapela, J. Percino, *Chem. Mater.* **2004**, *16*, 4634-4641. c) R. Kannan, G. S. He, L. Yuan, F. Xu, P. N. Prasad, A. G. Dombroskie, B. A. Reinhardt, J. W. Baur, R. A. Vaia, L.-S. Tan, *Chem. Mater.* **2001**, *13*, 1896-1904. d) B. A. Reinhardt, L. L. Brott, S. J. Clarson, A. G. Dillard, J. C. Bhatt, R. Kannan, L. Yuan, G. S. He, P. N. Prasad, *Chem. Mater.* **1998**, *10*, 1863-1874. e) H. M. Kim, B. R. Cho, *Chem. Commun.* **2009**, 153-164.

[9] K. Sonogashira, Y. Tohda, N. Hagihara, *Tetrahedron Lett.* **1975**, *50*, 4467-4470.

[10] Z. Pokladek, N. Ripoche, M. Betou, Y. Trolez, O. Mongin, J. Olesiak-Banska, K. Matczyszyn, M. Samoc, M. G. Humphrey, M. Blanchard-Desce, F. Paul, *Chem. Eur. J.* **2016**, *22*, 10155-10167.

[11] J. E. Rogers, J. E. Slagle, D. M. Krein, A. R. Burke, B. C. Hall, A. Fratini, D. G. McLean, P. A. Fleitz, T. M. Cooper, M. Drobizhev, N. S. Makarov, A. Rebane, K.-Y. Kim, R. Farley, K. S. Schanze, *Inorg. Chem.* **2007**, *46*, 6483-6494.

[12] E. J. Corey, P. L. Fuchs, *Tetrahedron Lett.* **1972**, 3769-3772.

[13] F. Paul, unpublished data.

[14] S. L. Streatfield, C. Pradels, A. Ngo Ndimba, N. Richy, A. Amar, A. Boucekkine, M. P. Cifuentes, M. G. Humphrey, O. Mongin, F. Paul, *Chem. Select.* **2017**, *2*, 8080–8085.

[15] L. J. Bellamy, The infrared spectra of complex molecules, Methuen & co Ltd, London, 1955.

[16] a) P. R. Bangal, D. M. K. Lam, L. A. Peteanu, M. J. van der Auweraer, *J. Phys. Chem. B* **2004**, *108*, 16834-16840. b) C. Katan, F. Terenziani, O. Mongin, M. H. V. Werts, L. Porrès, T. Pons, J. Mertz, S. Tretiak, M. Blanchard-Desce, *J. Phys. Chem. A* **2005**, *109*, 3024-3037. c) R. Stahl, C. Lambert, C. Kaiser, R. Wortmann, R. Jakober, *Chem. Eur. J.* **2006**, 2358-2370. d) F. Terenziani, C. Le Droumaguet, C. Katan, O. Mongin, M. Blanchard-Desce, *ChemPhysChem* **2007**, *8*, 723-734.

[17] a) B. Valeur, Molecular Fluorescence: Principles and Applications, Wiley-VCH Verlag GmbH, Weinheim, 2001, pp 125-154 and pp. 353-382. b) J. R. Lakowicz, Principles of Fluorescence Spectroscopy, 3rd edition, Springer Science, New York, 2006.

[18] a) E. Lippert, Z. Naturforsch. 1955, 10a, 541-545. b) N. Mataga, Y. Kaifu, M. Koizumi, *Bull. Chem. Soc. Jpn.* **1955**, *28*, 690-691.

[19] J. Dobkowski, J. Waluk, W. .Yang, C. Rullière, W. Rettig, *New J. Chem.* **1997**, *21*, 429-445.

[20] K. D. Belfield, M. V. Bondar, F. E. Hernandez, O. V. Przhonska, S. Yao, *J. Phys. Chem. B* **2007**, *111*, 12723-12729.

[21] Z. Pokladek, M. Dudek, O. Mongin, R. Métivier, P. Mlynarz, M. Samoc, K. Matczyszyn, F. Paul, *ChemPlusChem* **2017**, *82*, 1372-1383.

[22] For the compound **4-NMe$_2$"**, rotating one arm from 180 °C results in a decrease of the dipole moment from 4.15 D to 1.46 D.

[23] A. Beeby, K. Finlay, P. J. Low, T. B. Marder, *J. Am. Chem. Soc.* **2002**, *124*, 8280-8284 and refs therein.

[24] G. Grelaud, M. P. Cifuentes, F. Paul, M. G. Humphrey, *J. Organomet. Chem.* **2014**, *751*, 181-200.

[25] A. Triadon, G. Grelaud, N. Richy, O. Mongin, G. J. Moxey, I. M. Dixon, X. Yang, G. Wang, A. Barlow, J. Rault-Berthelot, M. P. Cifuentes, M. G. Humphrey, F. Paul, *Organometallics* **2018**, *35*, 2245-2262.

[26] A. Trujillo, R. Veillard, G. Argouarch, T. Roisnel, A. Singh, I. Ledoux, F. Paul, *Dalton Trans.* **2012**, *41*, 7454-7456.

[27] L. D. Lavis, R. T. Raines, *ACS Chem. Bio.* **2008**, *3*, 142-155

[28] G. Grelaud, M. P. Cifuentes, T. Schwich, G. Argouarch, S. Petrie, R. Stranger, F. Paul, M. G. Humphrey, *Eur. J. Inorg. Chem.* **2012**, 65-75.

[29] P. Jiang, Z. Wang, G. J. Moxey, M. Morshedi, A. Barlow, G. Wang, C. Quintana, C. Zhang, M. P. Cifuentes, M. G. Humphrey, *Dalton Trans.* **2019**, *48*, 12549-12559.

[30] a) N. Demas, G. A. Crosby, *J. Phys. Chem.* **1971**, *75*, 991-1024. b) G. R. Eaton, *Pure Appl. Chem.* **1988**, *60*, 1107-1114.

[31] B. Golec, M. Kijak, V. Vetokhina, A. Gorski, R. P. Thummel, J. Herbich, J. Waluk, *J. Phys. Chem. B* **2015**, *119*, 7283-7293.

[32] M. A. Albota, C. Xu, W. W. Webb, *Appl. Opt.* **1998**, *37*, 7352-7356.

[33] C. Xu, W. W. Webb, *J. Opt. Soc. Am. B* **1996**, *13*, 481-491.

[34] M. H. V. Werts, N. Nerambourg, D. Pélégry, Y. Le Grand, M. Blanchard-Desce, *Photochem. Photobiol. Sci.* **2005**, *4*, 531-538.

[35] C. Katan, S. Tretiak, M. H. V. Werts, A. J. Bain, R. J. Marsh, N. Leonczek, N. Nicolaou, E. Badaeva, O. Mongin, M. Blanchard-Desce, *J. Phys. Chem. B* **2007**, *111*, 9468-9483.

[36] M. Samoc, A. Samoc, B. Luther-Davies, M. G.Humphrey, M.-S. Wong, *Optical Materials* **2002**, *21*, 485-488.

[37] M. Sheik-Bahae, A. A. Said, T. Wei, D. J. Hagan, E. W. V. Stryland, *IEEE J. Quant. Electr.* **1990**, *26*, 760-769.

[38] M. J. Frisch, G. W. Trucks, H. B. Schlegel, G. E. Scuseria, M. A. Robb, J. R. Cheeseman, G. Scalmani, V. Barone, B. Mennucci, G. A. Petersson, H. Nakatsuji, M. Caricato, X. Li, H. P. Hratchian, A. F. Izmaylov, J. Bloino, G. Zheng, J. L. Sonnenberg, M. Hada, M. Ehara, K. Toyota, R. Fukuda, J. Hasegawa, M. Ishida, T. Nakajima, Y. Honda, O. Kitao, H. Nakai, T. Vreven, J. A. Montgomery (Jr.), J. E. Peralta, F. Ogliaro, M. Bearpark, J. J. Heyd, E. Brothers, K. N. Kudin, V. N. Staroverov, R. Kobayashi, J. Normand, K. Raghavachari, A. Rendell, J. C. Burant, S. S. Iyengar, J. Tomasi, M. Cossi, N. Rega, N. J. Millam, M. Klene, J. E. Knox, J. B. Cross, V. Bakken, C. Adamo, J. Jaramillo, R. Gomperts, R. E. Stratmann, O. Yazyev, A. J. Austin, R. Cammi, C. Pomelli, J. W. Ochterski, R. L. Martin, K. Morokuma, V. G. Zakrzewski, G. A. Voth, P. Salvador, J. J. Dannenberg, S. Dapprich, A. D. Daniels, Ö. Farkas, J. B. Foresman, J. V. Ortiz, J. Cioslowski, D. J. Fox, Gaussian 09 program (Revision A.2), Gaussian, Inc., Pittsburgh, PA, 2009.

[39] C. Adamo, V. Barone, *J. Chem. Phys.* **1998**, *108*, 664-675.

[40] J. Tomasi, B. Mennucci, R. Cammi, *Chem. Rev.* **2005**, *105*, 2999-3093.

[41] S. I. Gorelsky, SWizard program (Revision 4.5). ed., Available from: http:// www.sg-chem.net/, University of Ottawa, Canada, 2013.

[42] R. Dennington, T. Keith, J. Millam, GaussView program (Vers. 3.09), Semichem Inc., Shawnee Mission, KS, 2003.

Entry for the Table of Contents

Layout 1:

FULL PAPER

Molecular engineering allows for isolating strongly emissive triarylisocyanurates featuring large two-photon absorption cross-sections in the near-IR range. Remarkably, many of these cyclotrimeric chromophores depart from their octupolar symmetry after excitation their lowest singlet excitetd state in polar solvents.

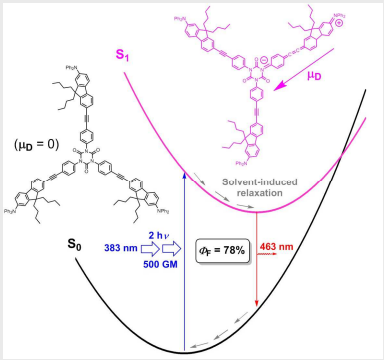

*Yohan Gauthier, Gilles Argouarch, Floriane Malvolti, Benjamin Blondeau, Nicolas Richy, Anissa Amar, Abdou Boucekkine, Krzysztof Nawara, Katarzyna Chlebowicz, Grażyna Orzanowska, Marek Samoc, Katarzyna Matczyszyn, Marta Ziemianek, Mireille Blanchard-Desce, Olivier Mongin, Jacek Waluk and Frédéric Paul**

Page No. – Page No.

Triarylisocyanurate-Based Fluorescent Two-Photon Absorbers